Doctoral Dissertation

Novel Bio-based Polymeric Materials from Bacterial Polyesters

Nao Hosoda

January, 2014

Graduate School of Engineering

Osaka University

Novel Bio-based Polymeric Materials from Bacterial Polyesters

Nao Hosoda

January 2014

Graduate School of Engineering

Osaka University

Contents

General Introduction

The evolution and the success of the chemical industry in the late 19th century were intimately related to the introduction of fossil feedstocks as a basis for synthesis. Today, fossil feedstocks in the form of oil and gas are by far the most important raw materials for the chemical industry, accounting for more than 90 %. The some parts of the raw materials are converted to polymers. Polymeric materials are widely utilized in every manufacturing industry, ranging from automobiles and medicines. The advantages of plastics, such as polypropylene (PP), polyethylene (PE), poly(vinyl chloride) (PVC), and polystyrene (PS) are their high strength, light weight, durability and low cost. More than 200 million tons of plastics are produced every year in the world[1,2]. However, contemporary geopolitical and economical developments have caused the disadvantages of a dependence on crude oil and its limited availability.[3] The ultimate formation of the greenhouse gas CO_2 from fossil feedstocks has unpredictable and irreversible consequences on the global climate. Furthermore, the plastic waste cannot be degraded by microorganisms and causes serious environmental problems.

Recently, the movement toward the resolution of environmental and resource issues in the world has been conducted. The concept of building a prosperous sustainable society was endorsed in the United Nations (UN) Earth Summit 2012 at Rio de Janeiro ("Rio + 20").[4] The prime objective of sustainable development, as stated by the Brundtland Commission of the UN General Assembly in 1987, implies meeting the needs of the present without compromising the ability of future generations to meet their own needs.[5] In sustainable society, it is imperative to reduce the demand for fossil resources and prevent environmental issues such as global warming. These elements are parts of sustainable chemistry, which are also referred to as green chemistry.[6] In polymer industry, one of the important ways is use of renewable resources as raw

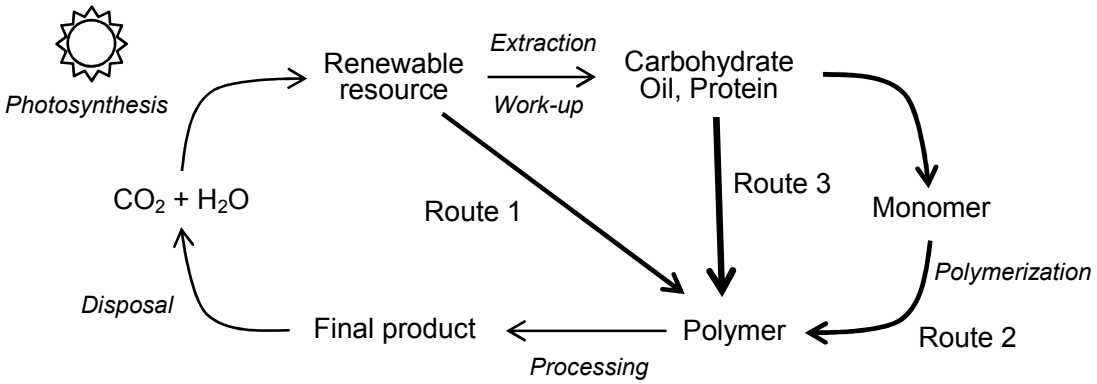

Figure 1. Schematic life-cycle of bio-based materials.

materials. Figure 1 shows the schematic life-cycle of bio-based materials. The materials from renewable resources are able to prevent the environmental issues in terms of greenhouse gas emission.

Bio-based polymers are divided by production method into the following three:

Route 1. Extraction from plants

Route 2. Combination of biological fermentation and chemical polymerization

Route 3. Fully microbial synthesis

Route 1 is a method by extraction from plants. Starch is prepared by this method and extracted from corn and crop. Starch has some advantages such as low cost and high biodegradability. Starch has been used as adhesives, binders, sizing material, glues and pastes.[7,8)]

Route 2 exhibits a method by microbial synthesis and chemical polymerization. Poly(L-lactic acid) (PLLA) is synthesized by ring opening polymerization from

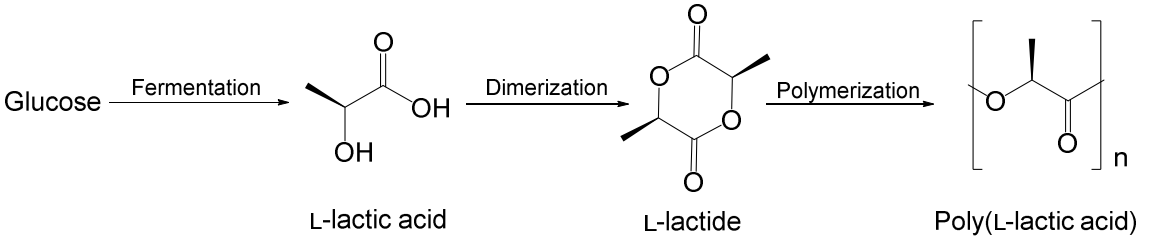

Scheme 1. Synthesis of poly(L-lactic acid).

L-lactide, which is a cyclic dimer of L-lactic acid obtained by fermentation (Scheme 1).[9] PLLA is one of the commercially available bio-based polymers.[10-12] It is a linear aliphatic thermoplastic with good biocompatibility, good transparency, and high strength and modulus.[13-17] Due to these properties, PLLA has attracted an interest in various fields, such as packaging, textile, and automobile.[18-20]

Route 3 is a microbial synthesis of polymers from renewable resources. In this method, the polymers are produced and accumulated in microorganisms. Polyhydroxyalkanoates (PHAs) are naturally-occurring polyesters that behave as intercellular energy-storage compounds in microorganisms, such as *Bacillus megaterium, Ralstonia eutropha,* and *Aeromonus cavie* (Figure 2).[21-23] These polymers have good biocompatibility and biodegradability. Therefore, applications of PHAs are expanded in various fields.[24]

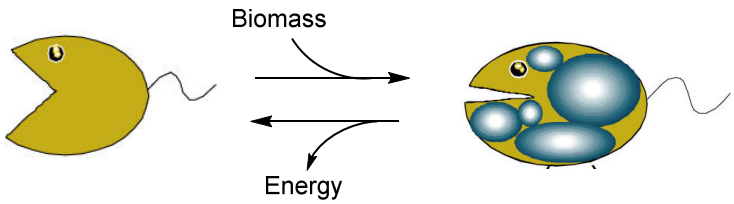

Figure 2. Microbial synthesis of polyhydroxyalkanoate.

In the 1920s, poly(3-hydoroxybutyrate) (PHB) was first isolated from *Bacillus megaterium* by Lemoigne.[25-31] Stanier and Wilkinson investigated the initial fundamental into the mechanisms of PHA biosynthesis in the late 1950s.[32),33] Poly(3-hydroxybutyrate-*co*-3-hydroxyvalerate) (PHBV) was found in activated sludge in 1974.[34] This is the first detection of PHA copolymer. Ballad and Doi investigated mechanism of biosynthesis of PHA in detail.[35,36] In 1993, poly(3-hydroxybutyrate-*co*-3-hydroxyhexanoate) (PHBH) was prepared by

fermentation.[37] The first industrial production of PHBV (Trade name of "Biopol") was carried out by Imperial Chemical Industries Co. (ICI) in the 1980s.[38),39)] Biopol was used as shampoo bottles and grips of the razor. However, the high cost and the brittleness resulted in limited application. Recently, Kaneka Co. produced PHBH, called "KANEKA biopolymer AONILEX", with a production capacity of 1000 tons per year (Figure 3).[40)]

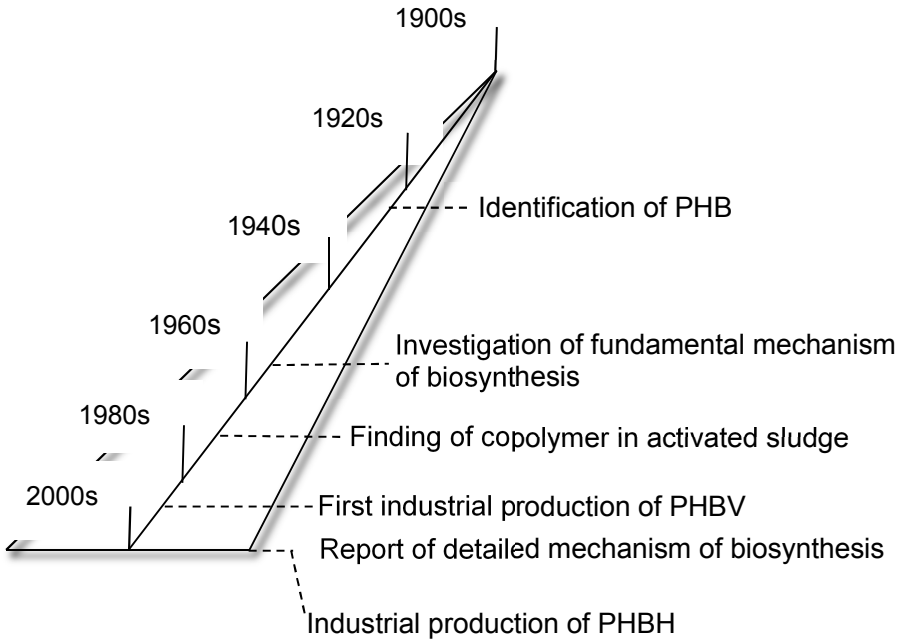

Figure 3. Development of PHA.

PHB, which is homopolymer of 3-hydroxybutyrate, is a crystalline polymer with glass transition temperature at 4 ºC and melting temperature at 180 ºC.[41-44)] Due to the high crystallinity, PHB has high tensile strength which is similar to PP. Elongation at break of PHB is 5%, although that of PP is more than 400%.[45,46)] The brittleness of PHB was attributed to large spherulite size and secondly crystallization. Thermal degradation temperature of PHB is close to its melting temperature. Therefore, PHB has narrow processing window. These disadvantages limited to application of PHB.[47-51)]

Nowadays, over 100 different types of PHAs are prepared by different bacterial species and fermentation conditions. Most of PHA copolymers consist of 3-hydroxybutyrate, which is main repeating unit, and another subunit (Figure 4). The PHA copolymers exhibit higher flexibility than PHB. It is possible to control the mechanical and thermal properties of PHA copolymers by the mole fractions. Generally, as the mole fractions of the subunit increased, the crystallinity and glass transition temperature decreased. Therefore, the copolymers become more flexible and tougher as the mole fraction of the subunit increased.[23,52] Diverse combination of the mole fractions offers a wide range of properties of PHAs compared with other bio-based polymers.[53] However, the applications of PHA copolymers are hindered by several disadvantages such as slow crystallization rate and relatively low mechanical strength.[23,54-59]

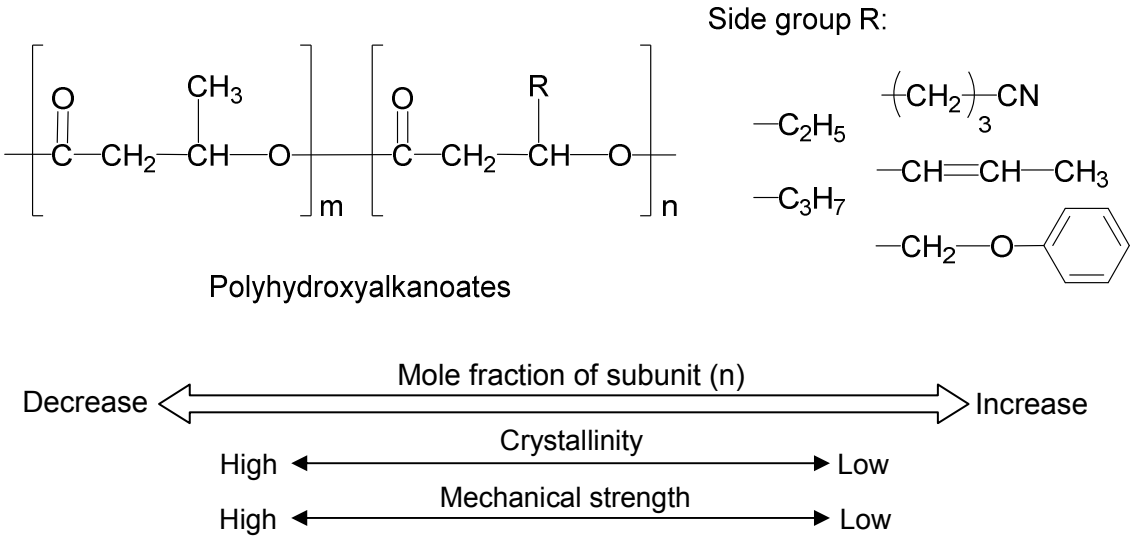

Figure 4. General chemical structure and properties of polyhydroxyalkanoates.

With the aforementioned background, the present thesis, "Novel Bio-based Polymeric Materials from Bacterial Polyesters", consists of three chapters including the following topics to develop green composites based on bacterial polyhydroxyalkanoates.

In Chapter 1, synthesis of plant oil-based green composites using porous PHB as a reinforcement material is described. Porous PHB was prepared by thermally-induced phase separation using dimethyl sulfoxide as a solvent. The acid-catalyzed curing of epoxidized soybean oil (ESO) was examined in the presence of the porous PHB, yielding a transparent composite (Figure 5). The mechanical properties of the ESO network polymer were improved by the incorporation of the porous PHB. The reinforcement effect of the porous PHB was investigated by dynamic viscoelasticity analysis and tensile test.

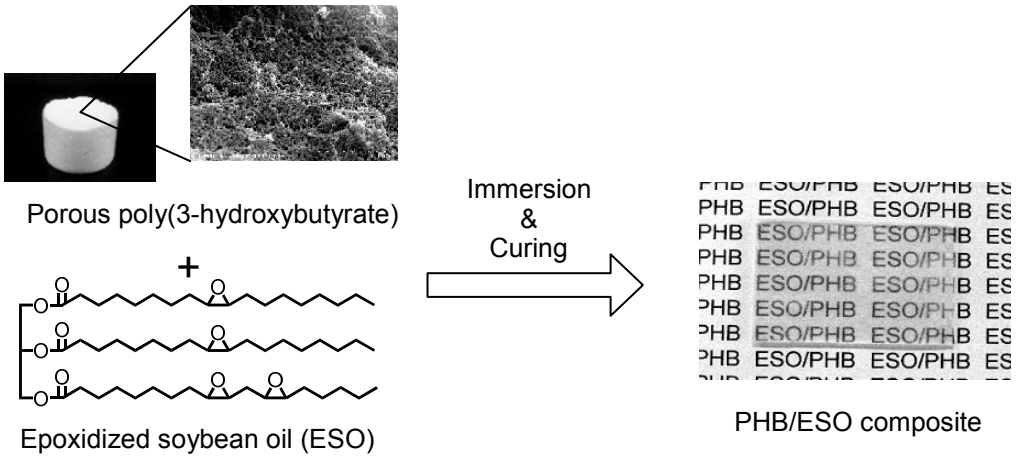

Figure 5. Preparation of plant oil-based green composite.

In Chapter 2, the effect of branched poly(lactic acid) bearing a castor oil core on crystallization of PHBV is mentioned. Small amount of the branched poly(lactic acid) accelerated the crystallization of PHBV (Figure 6). By the addition of the branched poly(lactic acid), the nuclear density of PHBV was dramatically increased. Moreover, the crystallization kinetic of PHBV was investigated.

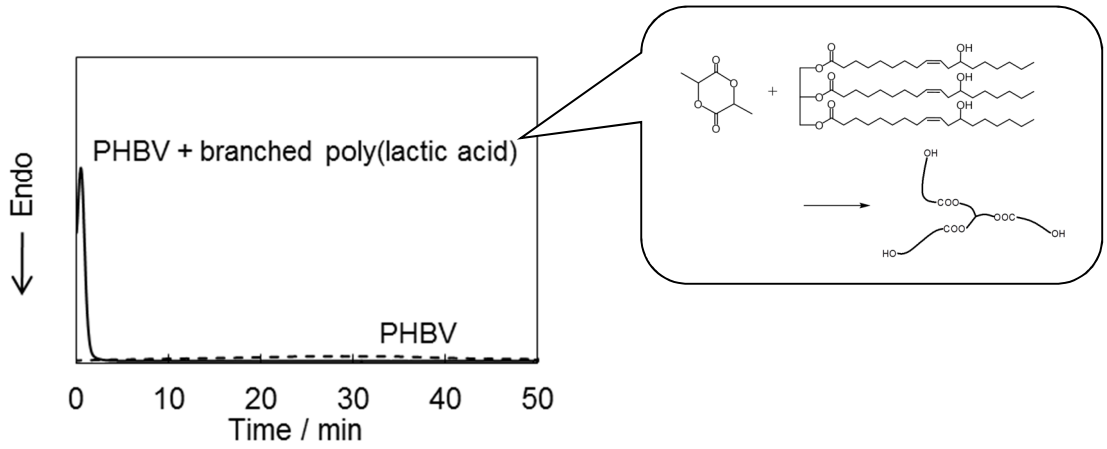

Figure 6. Effect of branched poly(lactic acid) on crystallization of PHBV.

In Chapter 3, preparation of green composites from PHBH and porous cellulose is described. Porous cellulose was prepared from precursor gel by using $Ca(SCN)_2$ aqueous solution as a solvent. The porous cellulose was impregnated with chloroform solution of PHBH and the subsequent drying produced a full bio-based composite, retaining the porous structure of cellulose. The resulting composites showed relatively good transparency (Figure 7). The mechanical properties of the composites were improved by the incorporation of the porous cellulose. Furthermore, the dimensional stability of the composites was investigated by thermal mechanical analysis.

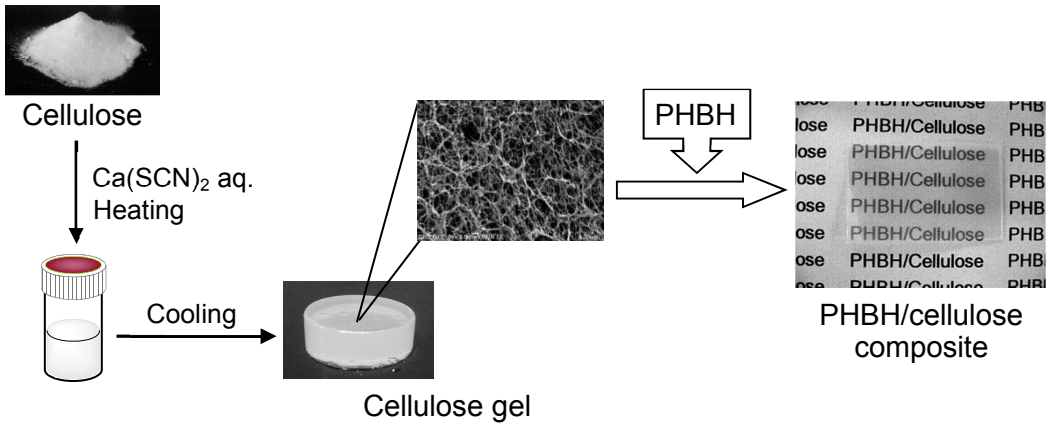

Figure 7. Synthesis of green composite of PHBH and porous cellulose.

Chapter 1

Plant Oil-based Green Composite Using Porous Poly(3-hydroxybutyrate)

Introduction

As discussed in General Introduction, poly(3-hydroxybutyrate) (PHB) is a highly crystalline and brittle polymer.[24, 48] The brittleness of PHB is caused by large spherulites and secondary crystallization. In order to overcome the shortcomings of PHB, PHA copolymers and the blend materials were developed.[41-44,49]

Plant oils, such as linseed, sunflower, soybean, and palm oils, are one of the most abundant renewable resources, and hence, are expected as an ideal alternative chemical feedstock.[1] Inexpensive triglyceride natural oils have been utilized extensively for coatings, inks, plasticizers, lubricants, resins, and agrochemicals in addition to their applications in food industry.[60-62] However, the low functionality and flexible aliphatic nature of plant oils result in several limitations for thermosets such as films with low mechanical properties.[63]

Epoxidized soybean oil (ESO) is manufactured by epoxidation of double bonds of soybean oil which is one of the lowest cost vegetable oils in the world, and it is industrially available in large volumes at a reasonable cost.[64] ESO is mainly used as a plasticizer for poly(vinyl chloride), chlorinated rubber, and poly(vinyl alcohol) emulsions to improve stability and flexibility.[65] Moreover, various cationic polymerization of epoxidized plant oils can be achieved by photoinitiators, latent catalysts, or acid catalysts. These epoxy compounds from renewable resources possess high potential as starting materials for bio-based thermosetting plastics.[66-71] Epoxidized plant oils were cured in the presence of inorganic chemicals to produce

organic-inorganic hybrid materials.[72-76] Furthermore, several researchers have investigated the plant oil-based green composites using kenaf, flax, hemp, and rosin derivatives as renewable compounds to improve poor mechanical properties.[77-80] Full bio-based composite was prepared by the curing of ESO in the presence of a PLLA nanofiber mat. The nano-scale structural control of the PLLA fiber mat improved the mechanical properties of the plant oil-based network polymer.[81]

Recently, Xin *et al*. have reported the fabrication of blend porous material of poly(3-hydroxybutyrate-*co*-3-hydroxyhexanoate) and polycarbonate.[82] This chapter deals with the synthesis of plant oil-based green composites using porous PHB as a reinforcement material for ESO-based network polymer. The porous PHB was prepared by thermally induced phase separation (TIPS). The resulting composites showed relatively good transparency with the improvement of mechanical properties.

Experimental

Materials

PHB (Mw= 1.4×10^5) was purchased from Sigma-Aldrich Co. (MO, USA). ESO and a thermally-latent cationic catalyst (benzylsulfonium hexafluoroantimonate derivative, Sun-Aid SI-60L) were gifts from Mizutani Paint Co. Ltd. (Osaka, Japan) and Sanshin Chemical Industry Co. Ltd. (Yamaguchi, Japan), respectively. Other reagents and solvents were commercially available and were used as received.

Synthesis of PHB/ESO composite

The following were typical procedures of the fabrication of PHB porous materials and the synthesis of PHB/ESO composites. PHB powder was dissolved in dimethyl sulfoxide (DMSO) at 90 ºC for 15 min, and the solution was cooled at room

temperature. After 5 h, the resulting white piece was washed with ethanol several times to obtain the porous PHB. For the synthesis of PHB/ESO composite, the porous PHB was immersed in ESO containing thermally-latent catalyst, followed by the vacuum treatment at room temperature to remove residual ethanol. Then, the sample was heated at 130 °C for 5 h to produce the PHB/ESO composite.

Measurements

Scanning electron microscopic (SEM) analysis was carried out by using a SU3500 instrument (Hitachi High-Technologies Co., Tokyo, Japan) at an accelerating voltage of 15 kV. Nitrogen adsorption-desorption isotherms were measured by a NOVA4200e (Quantachrome Co., FL, USA), and Brunauer-Emmett-Teller (BET) and Barrett-Joyner-Halendar (BJH) analyses were performed with the autosorb program. Fourier transform infrared (FT-IR) spectroscopy was recorded with a Nicolet iS5 (Thermo Fisher Scientific Inc., MA, USA). Thermogravimetric (TG) analysis was performed by using a TG/DTA7200 (Hitachi High-Tech Science Co., Tokyo, Japan) at a heating rate of 10 ºC/min under nitrogen. The thermal properties of the samples were measured under nitrogen atmosphere by a DSC6220 differential scanning calorimeter (DSC) (Hitachi High-Tech Science Co., Tokyo, Japan). The sample was cooled at -100 ºC for 2 min, and then heated to 200 ºC at a heating rate of 10 ºC/min. Dynamic viscoelasticity analysis was carried out by using a DMS6100 (Hitachi High-Tech Science Co., Tokyo, Japan) with frequency of 1 Hz at a heating rate of 3 ºC/min. Tensile properties were measured by a Shimadzu EZ Graph (Shimadzu Co., Kyoto, Japan) with a cross-head speed of 10 mm/min. The sample was cut into plate shape of 40 mm × 5 mm × 1 mm.

Results and Discussion

Fabrication of porous PHB material

A porous PHB was used as a reinforcement material for plant oil-based network polymer. Porous materials with a three-dimensional interconnected framework have many exciting properties, including high specific surface area, high permeability, low density, and fast mass transfer performance.[83)-91)] Owing to their properties, porous materials have received considerable attention in various fields such as chromatography, catalyst, and ion-exchange. The porous PHB was fabricated by TIPS method. PHB is insoluble in DMSO at room temperature but soluble by heating. PHB powder was dissolved in DMSO at 90 °C, followed by the cooling at room temperature and the washing with ethanol to form a white porous PHB retaining the shape of the vessel. Three samples of the porous PHB were prepared. The general procedure for the preparation of the porous PHB is illustrated in Figure 1-1. The morphology of the porous PHB was homogeneously macroporous with a three-dimensional interconnected fibrous structure, which is shown in Figure 1-2. This unique structure could be derived from a precursor gel and ascribed to the phase separation of the PHB/DMSO solution

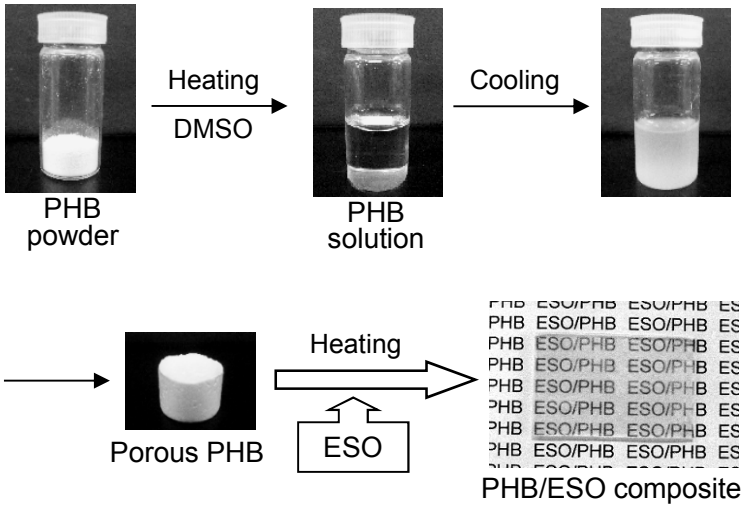

Figure 1-1. General procedure of preparations of porous PHB and PHB/ESO composite.

during the cooling process, where solvent-rich regions contributed to the porous formation. However, with the higher PHB concentration, some heterogeneous coagulations of PHB were observed (Figure 1-2(C)).

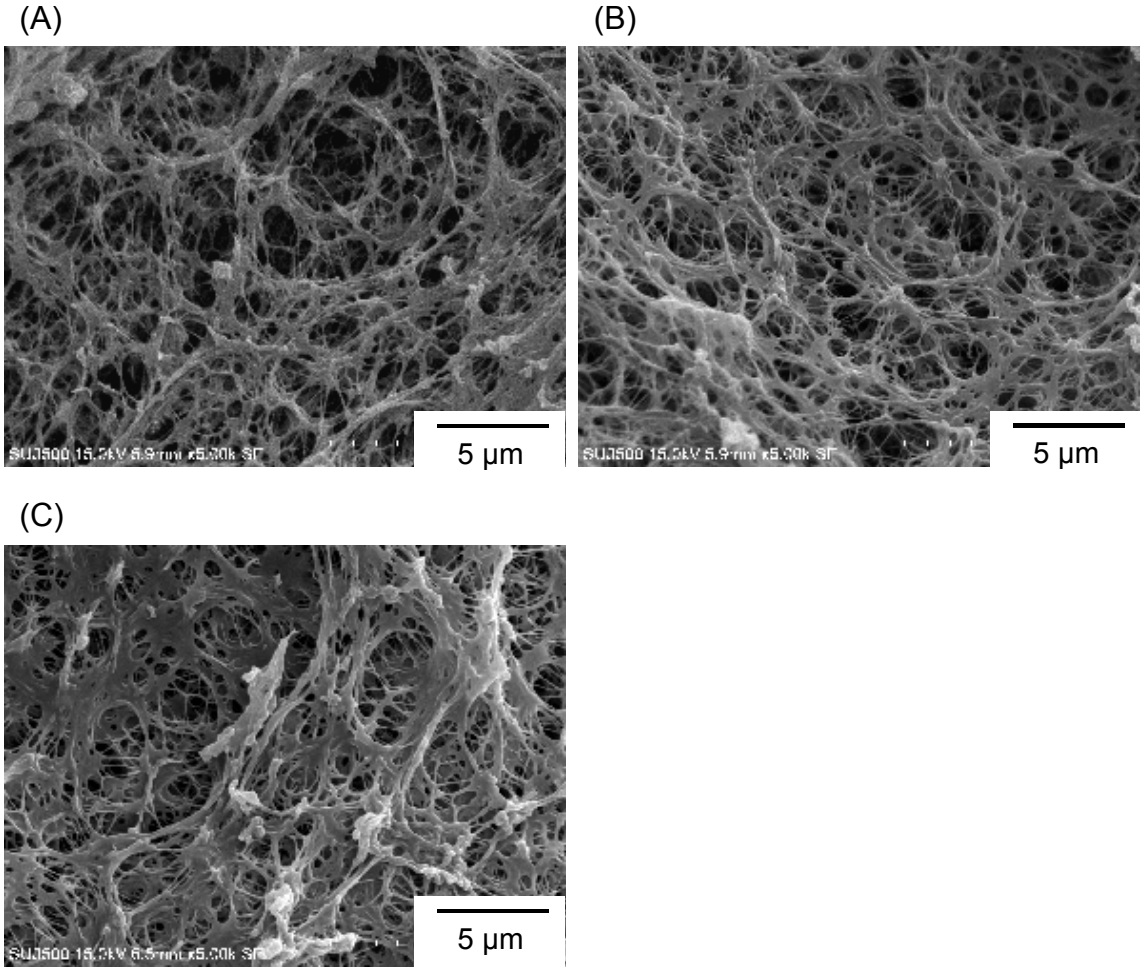

Figure 1-2. SEM images of porous PHB prepared from different concentrations of PHB in DMSO; (A) 50 $g \cdot L^{-1}$ (B) 100 $g \cdot L^{-1}$, and (C) 150 $g \cdot L^{-1}$.

Figure 1-3 shows the typical nitrogen adsorption-desorption isotherm of the porous PHB. The sharp nitrogen uptake near P_0 and the hysteresis loop in the P/P_0 range from 0.8 to 1.0 were observed, demonstrating the pore size distribution between mesopores and macropores. The surface area of the porous PHB, determined by BET

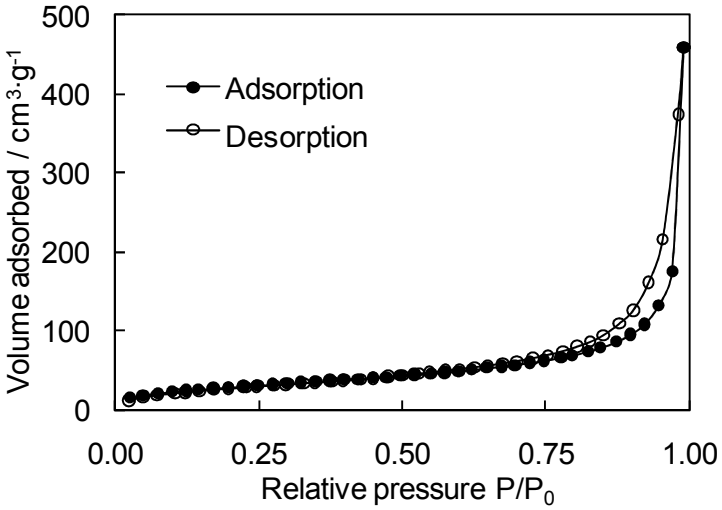

Figure 1-3. Typical nitrogen adsorption-desorption isotherm of porous PHB (PHB concentration: 100 $g \cdot L^{-1}$).

analysis, varied from 95 to 128 $m^2 \cdot g^{-1}$, and the formation of the porous PHB was dependent on the PHB concentration in DMSO (Table 1-1).

Synthesis of PHB/ESO composite

A PHB/ESO composite was prepared by immersion method. This relies on the penetration of ESO into the porous PHB by diffusion. The oxirane group number of

Table 1-1. Properties of porous PHB and PHB/ESO composite

Code	Porous PHB			Composite
	Concentration[a] / $g \cdot L^{-1}$	Surface area / $m^2 \cdot g^{-1}$	Pore volume / $cm^3 \cdot g^{-1}$	PHB content[b] / wt%
ESO homopolymer	–	–	–	0
PHB/ESO-50	50	128	0.52	5
PHB/ESO-100	100	107	0.71	11
PHB/ESO-150	150	95	0.33	19

[a] PHB concentration in DMSO.

[b] PHB content of PHB/ESO composite.

ESO used in this experiment was 3.7 per a molecule, determined by ^{1}H NMR spectroscopy. For the synthesis of PHB/ESO composites, the porous PHB was immersed in ESO containing thermally-latent catalyst, and the crosslinking of ESO was carried out at 130 °C which was below the melting temperature of PHB. The resulting composites showed relatively good transparency, suggesting the full impregnation of ESO and the uniform distribution of PHB in the ESO polymer. Figure 1-4 shows FT-IR spectra of ESO, porous PHB, and PHB/ESO composite. In the spectrum of the PHB/ESO composite, a peak at 823 cm^{-1} ascribed to C-C antisymmetric stretch of the oxirane groups of ESO was not observed, and a broad peak centered at 3400 cm^{-1} due to O-H vibration newly appeared. These data indicate that the oxirane groups are reacted with each other to form plant oil-based network structure. Moreover, two peaks at 1723 and 1743 cm^{-1} ascribed to C=O stretch of carboxyl groups of the ESO polymer and PHB were observed.

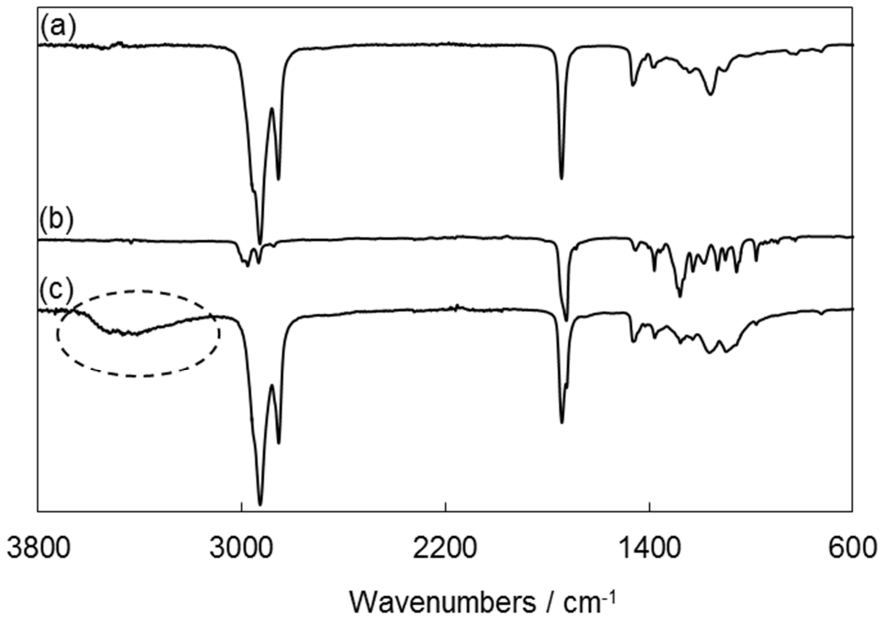

Figure 1-4. FT-IR spectra of (a) ESO, (b) porous PHB, and (c) PHB/ESO-100 composite.

Figure 1-5 represents the SEM images of the fracture surface of the ESO homopolymer and the PHB/ESO-100 composite. The ESO homopolymer was brittle, and the fracture occurred where a crack spread easily and freely. The fracture cross-section of the ESO homopolymer was smooth and uniform surface. On the other hand, the SEM image of the PHB/ESO-100 composite showed dense filling of fibrous protrusions attributed to the porous PHB.

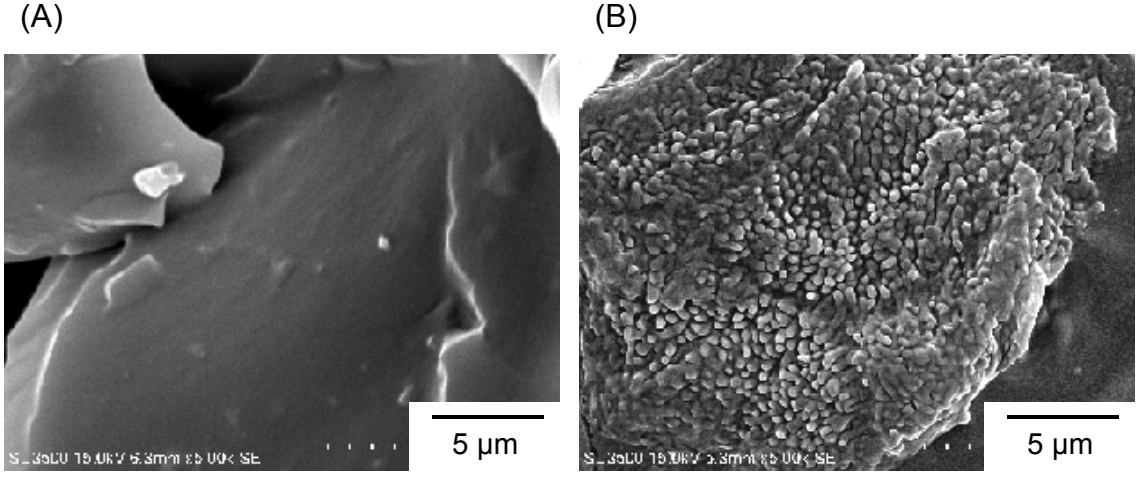

Figure 1-5. SEM images of cross-section of (A) ESO homopolymer and (B) PHB/ESO-100 composite.

Thermal properties of PHB/ESO composite

Thermal degradation of the ESO homopolymer, the porous PHB, and the PHB/ESO composites was studied by TG measurement (Figure 1-6). TG traces of the ESO homopolymer and the porous PHB showed only one weight-loss behaviors at 270 and 400 °C, respectively, due to the thermal decomposition. Almost no residues were observed at 500 °C. It was found that the PHB/ESO composites decomposed through two stage weight-loss processes, with the first weight-loss occurring at ca. 300 °C and the second one at ca. 400 °C. Comparing the traces of the PHB/ESO composites to those of the ESO homopolymer and the porous PHB, the first and second weight-losses

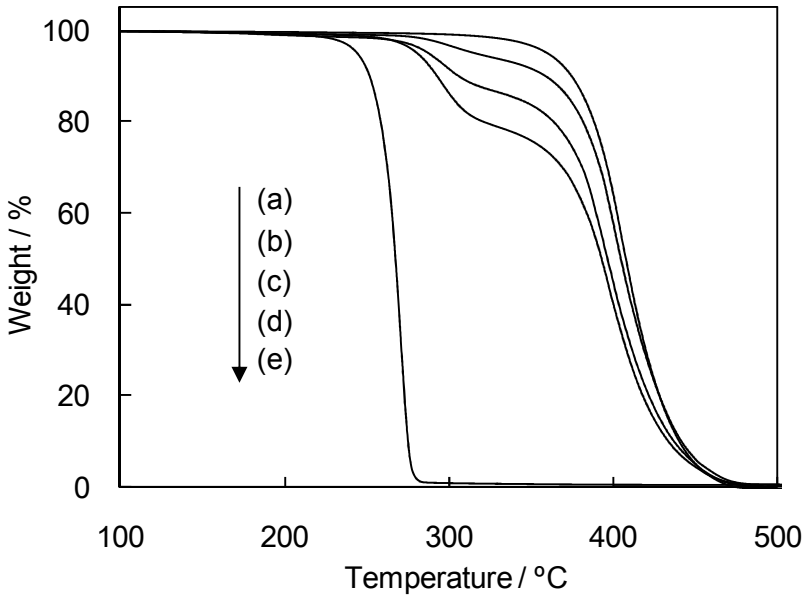

Figure 1-6. TG traces of (a) ESO homopolymer, (b) PHB/ESO-50, (c) PHB/ESO-100, (d) PHB/ESO-150 composites, and (e) porous PHB.

could be attributed to the decomposition of PHB and ESO components, respectively. Therefore, TG analysis allowed the assessment of PHB content of the composites from the first weight-loss (Table 1-1). The PHB content of the composites increased as a function of the PHB concentration in DMSO. The first decomposition temperature of the PHB/ESO composites was slightly higher than that of the porous PHB, suggesting that the ESO polymer prevents out diffusion of volatile decomposition products.[92,93)]

The PHB/ESO composite was soaked in chloroform for 24h. The PHB component was dissolved in chloroform, and the residue weight was close to the ESO content obtained by TG measurement. In the SEM image of the residue after soaking of the composite, the pores derived from the depletion of PHB were observed. These results indicate that the porous structure of PHB is retained without shrinkage during the synthesis of the composite.

DSC measurement of the ESO homopolymer, the porous PHB, and the PHB/ESO-100 composite was carried out to evaluate the effect of the porous PHB on the thermal behaviors (Figure 1-7). In the first heating curve of the ESO homopolymer, only a glass transition was observed at -34 °C, whereas the curve of the porous PHB showed a glass transition and melting of PHB at -16 and 168 °C, respectively. In the curve of the PHB/ESO-100 composite, two glass transitions ascribed to the ESO polymer and PHB were observed at -45 and -18 °C, respectively. These data indicates that most of the PHB components are immiscible to the ESO polymer. The crystallinity of the PHB component in the PHB/ESO-100 composite was about 60 %, and this value hardly changed compared with that of the porous PHB (64 %). Furthermore, both curves of the ESO homopolymer and the PHB/ESO composite were almost constant in the higher temperature region, suggesting the quantitative consumption of the oxirane groups of ESO.

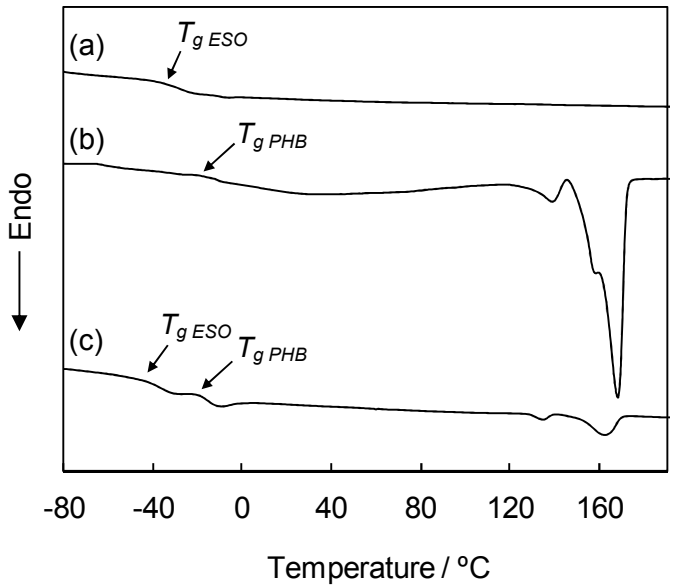

Figure 1-7. DSC curves of first heating scan for (a) ESO homopolymer, (b) porousPHB, and (c) PHB/ESO-100 composite.

Mechanical properties of PHB/ESO composite

Figure 1-8 shows the dynamic viscoelasticity (storage modulus and loss factor) as a function of temperature for the ESO homopolymer and the PHB/ESO-100 composite. For both samples, the storage moduli remained almost constant at low temperature between -100 and -60 °C, and dropped as temperature increased. In the rubbery region, the storage modulus of the PHB/ESO composite was higher than that of the ESO homopolymer, suggesting the reinforcement effect of the crystallized PHB. A broad peak of the loss factor of the ESO homopolymer was found around 0 °C, which was regarded as the α-transition corresponding to the glass transition of the ESO polymer. The α-transition of the PHB/ESO composite shifted to a lower temperature region. This may be because the distances between crosslinked points become longer by the incorporation of the porous PHB. Moreover, a small peak newly appeared at 25 °C, which corresponded to the glass transition of PHB. This result is in good agreement with DSC analysis.

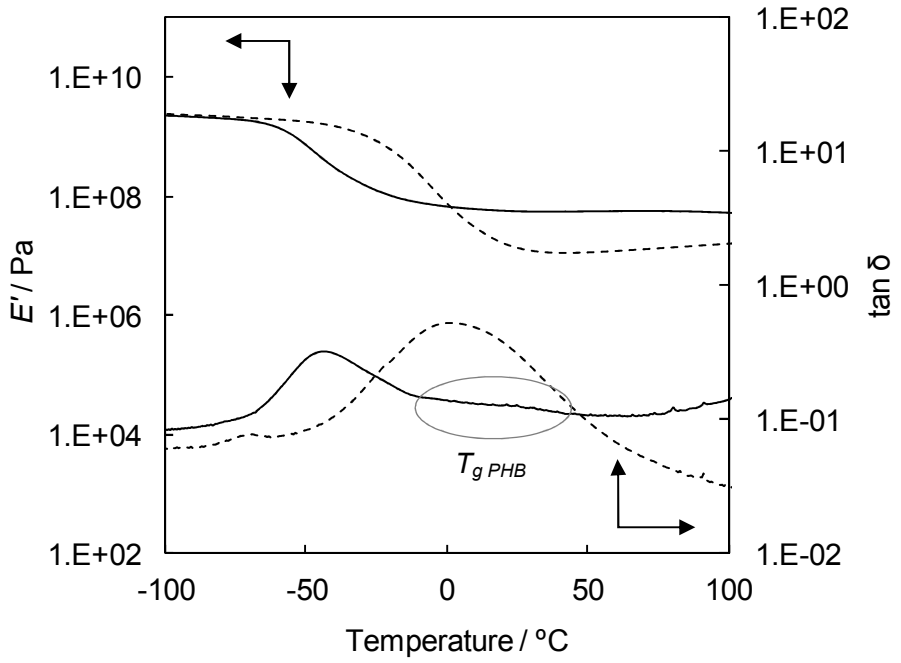

Figure 1-8. Dynamic viscoelasticity of ESO homopolymer and PHB/ESO-100 composite.

To evaluate the reinforcement effect of the porous PHB, tensile test was performed. The strain-stress curves of the ESO homopolymer and the PHB/ESO composites are shown in Figure 1-9. The porous PHB was too brittle to be carried out the tensile test. Mechanical properties of fiber-reinforced materials are affected by some

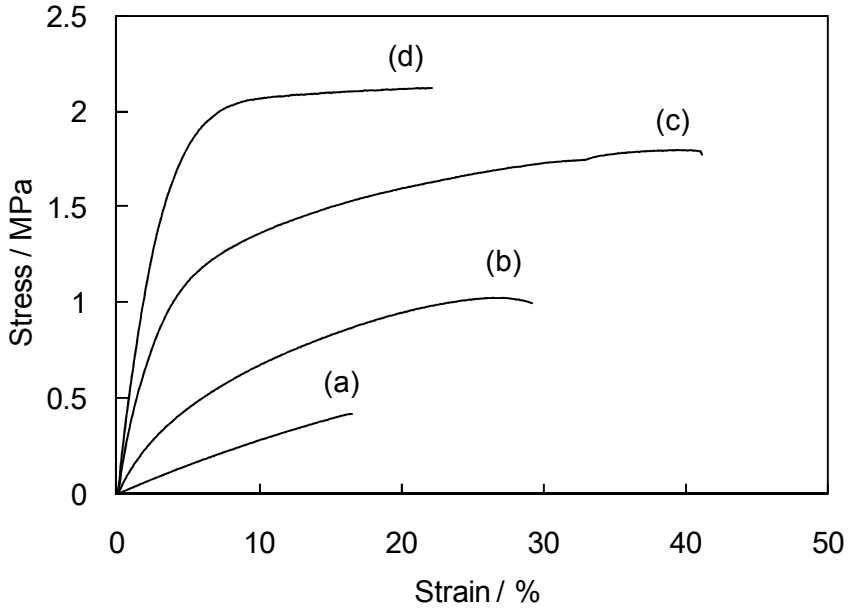

Figure 1-9. Strain-stress curves of (a) ESO homopolymer, (b) PHB/ESO-50, (c) PHB/ESO-100, and (d) PHB/ESO-150 composites.

factors such as fiber volume, aspect-ratio, fiber-matrix adhesion, and orientation. Tensile strength and toughness are dependent on the compatibility between fiber and the matrix, while modulus is influenced by fiber impregnation or aspect-ratio of fiber.[94] The incorporation of the porous PHB increased the Young's modulus and tensile strength, compared with those of the ESO homopolymer. These data indicate the good distribution of the PHB component in the ESO polymer. Moreover, the strain at break of the PHB/ESO composites was larger than that of the ESO homopolymer. Plant oils are often used as a plasticizer for biopolymers such as poly(lactic acid) and PHAs.[95-98] The three-dimensional fibrous structure of PHB improved the brittleness of ESO-based network polymer and PHB, due to the good interfacial adhesion and the formation of

the interaction between the ESO chains and the surface of the porous PHB. The improvement effect of the mechanical properties was dependent on the PHB content of the composites. The Young's modulus and tensile strength of the composites increased as the PHB content increased. On the other hand, the largest strain at break was found in the PHB/ESO-100 composite. The decrease of the strain at break in the PHB/ESO-150 composite may be due to the aggregation of PHB during phase separation process (see Figure 1-2(C)). Moreover, the toughness of the PHB/ESO composites, defined as the area of the strain-stress curve, was much larger than that of the ESO homopolymer. This data implies that the resulting composites possess great capacity to absorb energy before breaking.

Conclusions

A porous PHB was fabricated by TIPS method using DMSO as a solvent to produce a piece of white material with a three-dimensional interconnected fibrous structure. By changing the concentration of PHB in DMSO, the formation and structure of the porous PHB could be easily controlled. The porous PHB was immersed in ESO with thermally-latent catalyst, and the subsequent curing of ESO gave the PHB/ESO composite. The resulting composites were relatively transparent, due to the nano-scale fibrous structure of PHB. DSC and DMA results of the composite showed two glass transitions and the melting of PHB. The Young's modulus and the tensile strength of the PHB/ESO composites were larger than those of the ESO homopolymer. The incorporation of the porous PHB also increased the strain at break, indicating the resulting composites are effectively reinforced without sacrificing toughness.

Chapter 2

Crystallization Behavior of Poly(3-hydroxybutyrate-*co*-3-hydroxyvarelerate) Adding Branched Poly(lactic acid) as a Nucleating Agent

Introduction

Poly(3-hydroxylbutyrate) (PHB) has potential applications in packaging, coating, agricultural films, etc.[45-51] However, the application of these materials is hindered by some disadvantages such as the narrow processing window, poor thermal stability, and high brittleness.[99-104] Considerable effort has been expended to solve these problems and to improve the physical properties of PHB. Strategies including blending of PHB with other polymers,[105-108] annealing of the molding articles,[109] and copolymerization of 3-hydroxybutyrate (3-HB) with another subunit have been undertaken.[41),42] The higher ductility of poly(3-hydroxybutyrate-*co*-3-hydroxyvalerate) (PHBV) relative to the PHB homopolymer makes it of particular importance among these copolymers. However, PHBV has a slow crystallization rate, and these properties become more detrimental with an increase in 3-hydroxyvalerate (3-HV) unit content. Because of the low crystallization rate, the films made from PHBV are tacky with a tendency of self-adhesion. In addition, a large fraction of the subunit remains amorphous and undergoes crystallization slowly during storage.[110] Therefore, acceleration of the crystallization of these copolymers by addition of a nucleating agent is of prime importance. Many kinds of nucleating agents have been proposed for PHB and the copolymers, including talc, boron nitride, saccharin, lignin, terbium oxide, lanthanum oxide, melamine, uracil, metal phosphate, α-cyclodextrin, and organophosphorous compounds.[111-121] Although the addition of such nucleating agents has resulted in an increased crystallization rate, some of these components are

undesirable in finished articles that may come into contact with humans, animals, or the environment.

Recently, branched poly(lactic acid) bearing a castor oil core was synthesized and its pasticization effct on poly(L-lactic acid) (PLLA) was reported. The addition of only a small amount of the branched poly(lactic acid) to PLLA exerted a plasticization effect and suppressed the lowering of the tensile strength and the thermal properties of PLLA.[122] This chapter deals with development of novel nucleating agent for PHBV. The crystallization behavior of PHBV was investigated in the presence of the branched poly(lactic acid) as a nucleating agent, via differential scanning calorimetry (DSC) and polarized optical microscopy (POM). The study, wich was described in this chapter, has considerable significance for the development of biomass plastics based on the bio-based additive consisting of castor oil and lactide presented herein.

Experimental

Materials

PHBV containing 5 mol% 3-HV (Mw= 5.0×10^5) was purchased from Sigma-Aldrich Co. (CO., USA). Castor oil was obtained from Wako Pure Chemical Industries, Ltd., (Osaka, Japan) and L- and D,L-lactides were purchased from Tokyo Kasei Co. (Tokyo, Japan), and used without further purification. Other reagents and solvents were commercially available and were used as received.

Synthesis of branched poly(lactic acid)s

The following procedure was typically used in the synthesis of branched poly(lactic acid).[122] A mixture of L-lactide (LLA) (0.72 g, 5.0 mmol), castor oil (0.093 g, 0.1 mmol), and tin (II) octanoate (2.0 mg, 5.0×10^{-3} mmol) was kept under argon

atmosphere at 130 °C with gentle stirring. After 24 h, the mixture was dissolved in 3 mL of chloroform, and the solution was poured into 60 mL of ethanol. The precipitated polymeric material was collected by centrifugation and dried *in vacuo* to yield 0.63 g of the polymer (78 % yield). Linear poly(lactic acid) (LP-L25) was synthesized by a similar procedure using 1-octanol as an initiator.

Sample preparation of PHBV/branched poly(lactic acid) blend

PHBV (0.50 g) and branched poly(lactic acid) (0.025 g) were dissolved in 10 mL of chloroform at room temperature with gentle stirring. After 12 h, the solution was cast on a glass plate, and the solvent was allowed to evaporate for 12 h at room temperature. The obtained solid was heated at 175 °C for 10 min, and hot pressed at 175 °C under a pressure of 5 MPa for 20 min. This was followed by rapid quenching at 0 °C to produce a blended sample.

Measurement

^{1}H nuclear magnetic resonance (NMR) spectra were recorded on a Bruker DPX-400 instrument (Bruker BioSpin Co., MA, USA). Size-exclusion chromatographic (SEC) analysis was carried out at 40 °C using a TOSOH SC8020 apparatus with a refractive index detector and a TOSOH TSKgel G3000$_{HHR}$; the eluent used was chloroform at a flow rate of 1.0 mL/min (Tosoh, Tokyo, Japan). A calibration curve was obtained using polystyrene standards.

Polarized microscopic analysis was carried out using an OLYMPUS BX51 microscope (Olympus, Tokyo, Japan) equipped with an IMOTO MHS-2000 heating stage (Imoto Machinery, Kyoto, Japan). The sample was placed on a glass slide, melted at 180 °C on a heating stage, and subsequently cooled at room temperature.

The crystallization behavior of the samples was investigated under nitrogen atmosphere using a SEIKO DSC6020 differential scanning calorimeter (DSC) (Hitachi High-Tech

Science Co., Tokyo, Japan). For the non-isothermal crystallization, the sample was melted at 180 °C for 15 min and then cooled to -50 °C at a cooling rate of 10 °C/min. The temperature was maintained for a duration of 15 min, and the sample was reheated to 180 °C at a heating rate of 10 °C/min. For isothermal crystallization, the sample was first heated to 180 °C for 15 min, and the temperature was rapidly decreased (100 °C/min) to the predetermined crystallization temperature. The temperature was then held constant until the completion of crystallization.

Results and discussion

Synthesis of branched poly(lactic acid) bearing castor oil core

Branched poly(lactic acid)s were synthesized from castor oil and lactide by ring-opening polymerization using tin (II) octanoate as a catalyst.[122)] Castor oil, which has three secondary hydroxyl groups, was used as an initiator for the polymerization of

Table 2-1. Properties of linear poly(lactic acid) and branched poly(lactic acid)s

Code	Lactide	Feed [a] ratio	M_n [b]	M_w/M_n [b]	T_g [c] / °C	T_m [c] / °C
LP-L25	L-lactide	25	4100	1.8	11.0	54.0
BP-L25	L-lactide	25	5500	1.4	8.1	143.2
BP-DL25	D,L-lactide	25	5700	1.3	4.8	— [d]
BP-L50	L-lactide	50	9600	1.3	10.4	151.5
BP-DL50	D,L-lactide	50	8900	1.2	15.0	— [d]
BP-L75	L-lactide	75	12500	1.4	13.3	156.8
BP-L100	L-lactide	100	14800	1.6	19.5	161.3

[a] Lactide/initiator (mol/mol).

[b] Determined by SEC.

[c] Determined by DSC.

lactide. Six branched and one linear poly(lactic acid)s were prepared as nucleating agents for PHBV (Table 2-1). The molecular weight of the branched poly(lactic acid)s was quite close to the value calculated based on the feed ratio. Thus, the feed ratio was used as a measure of the molecular weight of the branched poly(lactic acid) in the evaluation of the nucleation effects.

Non-isothermal crystallization

The effects of the branched poly(lactic acid) on the crystallization of PHBV were investigated by DSC measurements. Generally, a high melt crystallization temperature is taken as an indicator of fast crystallization during non-isothermal crystallization. Figure 2-1 shows the non-isothermal melt crystallization and the melting behaviors of neat PHBV, PHBV/LP-L25, PHBV/BP-L25, and PHBV/BP-DL25 blends. The crystallization rate of the neat PHBV was very slow, and no melt crystallization peak was observed during the cooling process at 10 °C/min (Figure 2-1(A)). In the subsequent heating process, a cold crystallization peak appeared in the temperature

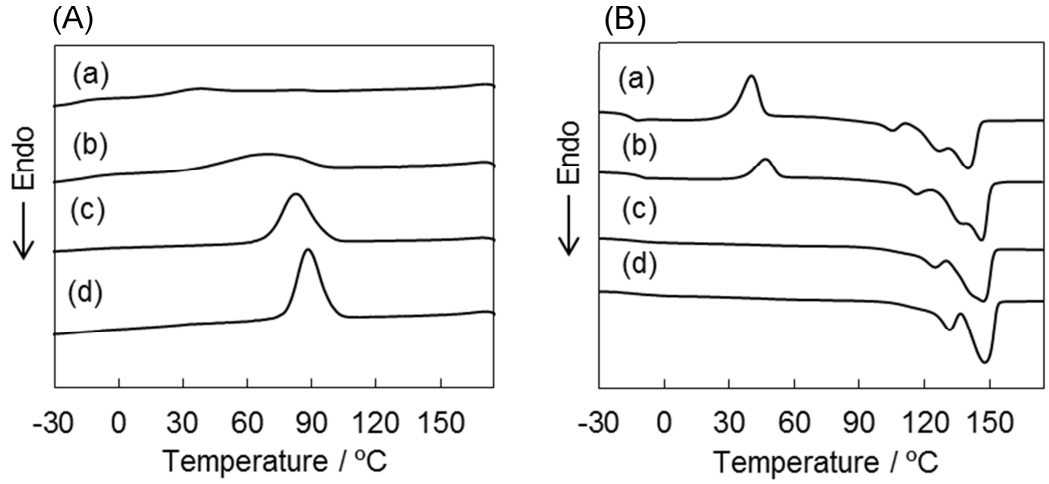

Figure 2-1. DSC curves of (A) non-isothermal crystallization and (B) subsequent heating scans for (a) neat PHBV, (b) PHBV/LP-L25 (5 wt%), (c) PHBV/BP-L25 (5 wt%), and (d) PHBV/BP-DL25 (5 wt%) blends. Both the cooling and the heating rates are 10 ºC/min.

range of 30 to 50 °C (Figure 2-1(B)). The DSC curves of the PHBV/LP-L25 blend were similar to those of neat PHBV. Although the crystallization of PHBV was slightly accelerated by the incorporation of LP-L25, crystallization of the PHBV/LP-L25 blend could not be complete during the cooling process at 10 °C/min. On the other hand, with the addition of the branched poly(lactic acid), melt crystallization peaks appeared at the higher temperature of ca. 80 °C and became much sharper than that of the PHBV/LP-L25 blend. The crystallization peaks of the PHBV/BP-L25 and PHBV/BP-DL25 blends were not observed in the subsequent heating scan because most of the PHBV crystallized during the cooling process. These data indicate that the branched poly(lactic acid) accelerates the crystallization of PHBV significantly, and the nucleation effect exerted by these additives are greater than that of the linear poly(lactic acid). This may be that the branched poly(lactic acid) having the castor oil core was well-dispersed in PHBV matrix than the linear poly(lactic acid), because plant oil acts as a plasticizer of PHA in microorganisms.[123)]

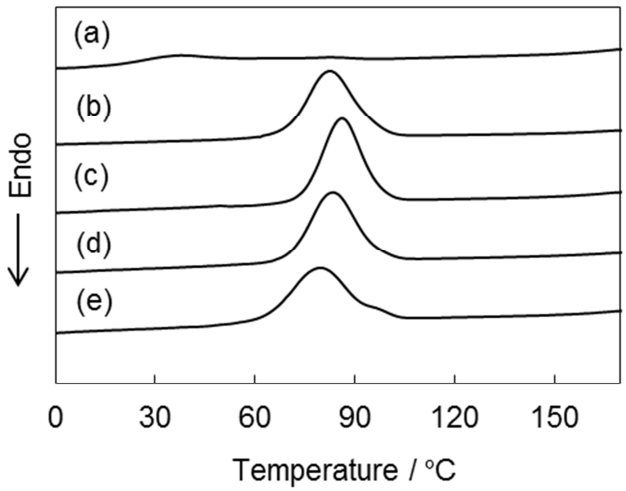

Figure 2-2. DSC curves of non-isothermal crystallization at a cooling rate of 10 ºC/min; (a) neat PHBV, (b) PHBV/BP-L25, (c) PHBV/BP-L50, (d) PHBV/BP-L75, and (e) PHBV/BP-L100 blends. Additive amount of the branched poly(lactic acid) are 5 wt%.

Figure 2-2 shows the DSC analysis of the melt crystallization behaviors of neat PHBV and PHBV/branched poly(lactic acid) blends with different molecular weights (i.e., feed ratio of lactide to castor oil). It is obvious that the branched poly(lactic acid)s were able to enhance the crystallization of PHBV to a significant degree during the cooling process at 10 °C/min, compared with neat PHBV. The melt crystallization temperature (T_{mc}) was dependent on the molecular weight of the branched poly(lactic acid)s, and the highest T_{mc} was found for the PHBV/BP-L50 blend.

All parameters derived from the DSC curves, i.e., T_{mc}, the enthalpy of melt crystallization (ΔH_{mc}), the glass transition temperature (T_g), the cold crystallization temperature (T_{cc}), the enthalpy of cold crystallization (ΔH_{cc}), the melting temperature (T_m), and the melting enthalpy (ΔH_m) of neat PHBV, PHBV/linear poly(lactic acid) and PHBV/branched poly(lactic acid) blends are summarized in Table 2-2. By the addition

Table 2-2. Non-isothermal crystallization and melting behaviors of PHBV, PHBV/linear poly(lactic acid), and PHBV/branched poly(lactic acid) blends

Code	Content [a] / wt%	T_{mc} / °C	ΔH_{mc} / J·g^{-1}	T_g / °C	T_{cc} / °C	ΔH_{cc} / J·g^{-1}	T_m / °C	ΔH_m / J·g^{-1}
PHBV	0	38.4	6.1	-19.2	40.6	36.4	140.2	64.9
PHBV/ BP-L25	5	82.4	59.2	-19.5	— [b]	— [b]	146.3	65.9
PHBV/ BP-L50	2.5	83.2	63.5	-19.4	— [b]	— [b]	145.4	69.8
PHBV/ BP-L50	5	86.2	62.8	-19.2	— [b]	— [b]	145.2	72.0
PHBV/ BP-DL50	5	93.9	66.3	-19.2	— [b]	— [b]	150.1	68.4
PHBV/ BP-L50	7.5	84.0	54.4	-19.2	— [b]	— [b]	148.1	62.2
PHBV/ BP-L50	10	71.2	43.3	-18.9	43.7	6.6	145.9	69.7
PHBV/ BP-L75	5	83.8	60.3	-19.3	— [b]	— [b]	147.0	69.0
PHBV/ BP-L100	5	79.5	58.1	-19.2	— [b]	— [b]	146.9	70.2

[a] Content of poly(lactic acid) for PHBV.

[b] Not observed.

of the branched poly(lactic acid), the crystallization parameters changed significantly compared with those of the melting ones. Remarkable crystallization of PHBV was achieved during the cooling scan by the addition of even 2.5 wt% of BP-L50. The T_m and ΔH_m of PHBV/branched poly(lactic acid) blends were slightly higher than those of neat PHBV, and the T_g of the PHBV/branched poly(lactic acid) blends changed negligibly in comparison to that of neat PHBV. The T_g provides useful information on blend miscibility. If the blend is one phase (miscible), a single T_g lying between the values for each component is detected. If the blend is two phase (immiscible), two T_g are observed close to or matching those of the two components.[124,125] The T_g of the BP-L50 was slightly observed around 10 °C in PHBV/BP-L50 blend. The crystallization of PHBV was also accelerated by the addition of BP-DL50, which is an amorphous polymer. These data suggest that the branched poly(lactic acid) enhances the overall crystallization due to the heterogeneous nucleation function by phase separation.

Isothermal crystallization

In order to understand the effect of the branched poly(lactic acid) on the crystallization rate of PHBV, the isothermal crystallization behavior of neat PHBV and PHBV/branched poly(lactic acid) blends was investigated. Figure 2-3 shows typical isothermal crystallization curves for neat PHBV, PHBV/BP-L50, and PHBV/BP-DL50 blends. The crystallization rate of neat PHBV was extremely slow, and the crystallization was not completed within 60 min at 95 °C. With the addition of the branched poly(lactic acid), the exothermic peaks derived from crystallization became sharp, and the crystallization times were shorter than that of neat PHBV.

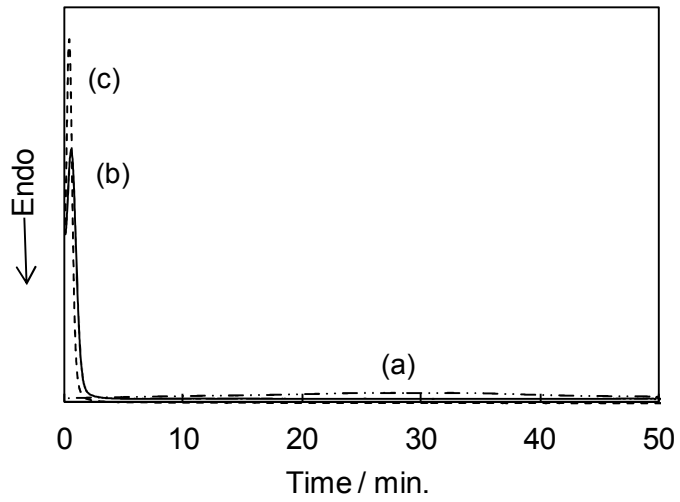

Figure 2-3. Typical isothermal crystallization curves of (a) neat PHBV, (b) PHBV/BP-L50 (5 wt%), and (c) PHBV/BP-DL50 (5 wt%) blends.

The well-known Avrami equation (Eq. (1)) is often used to analyze the isothermal crystallization kinetics.[126-128)]

$$1 - X_t = \exp(-k \cdot t^n) \qquad (1)$$

Here, X_t is the relative degree of crystallinity at a certain time t, k is the overall crystallization rate constant that includes contributions from nucleation and growth rate, and n is the Avrami exponent, which depends on the nucleation and growth mechanism. If Eq. (1) is transformed into the double-logarithmic form, the equation of a straight line (Eq. (2)) is obtained, and the parameters k and n are determined from the intercept and the slope, respectively.

$$\log [-\ln (1 - X_t)] = \log k + n \log t \qquad (2)$$

When $X_t = 0.5$ in Eq. (2), the crystallization half time ($t_{1/2}$), which is the time taken for 50% of total-volume crystallization, is given as follows:

$$t_{1/2} = (\ln 2 / k)^{1/n} \qquad (3)$$

The Avrami double-logarithmic plots are shown in Figure 2-4, and the Avrami parameters calculated from these plots are shown in Table 2-3. Generally, the $t_{1/2}$ values increase with increasing temperature. In all of the samples evaluated, the $t_{1/2}$ values of

the PHBV/BP-L50 blends were lower than those of neat PHBV; this indicates rapid crystallization by the incorporation of BP-L50. Each curve in Figure 2-4 is characterized by an initial linear portion during the early stage of crystallization and a tendency for the slope to change due to secondary crystallization in the final stage. This secondary crystallization is considered to be the result of the spherulite impingement.

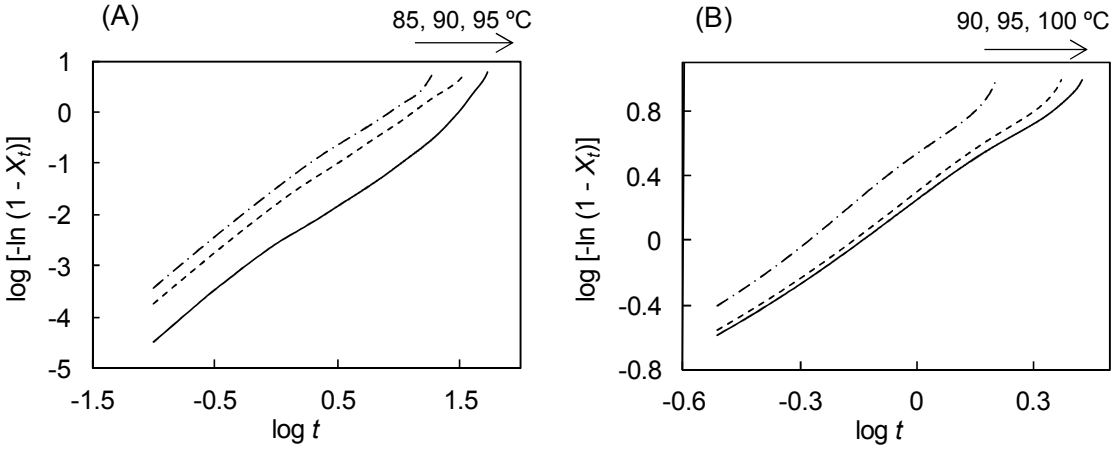

Figure 2-4. Isothermal Avrami plots of (A) neat PHBV and (B) PHBV/BP-L50 blend (5 wt%).

The n values of neat PHBV and PHBV/BP-L50 blends were in the range of 1.64 to 1.67 and 1.71 to 1.88, respectively, and were almost independent of the given isothermal crystallization temperature. The addition of BP-L50 increased the n values of the PHBV/BP-L50 blends. This increase in the n values may be attributed to the transition of the crystallization mechanism from diffusion control to contact control.[129,130] Similar behaviors were observed for the PHBV/BP-DL50 blends. The k values of the PHBV/BP-L50 and PHBV/BP-DL50 blends increased by more than two orders of magnitude relative to those of neat PHBV, indicating that the crystallization rate increased remarkably.

Table 2-3. Crystallization kinetic parameters and crystallization half time

Code	Temperature[a] / °C	n	k / min^{-n}	$t_{1/2}$ / min
PHBV	85	1.67	0.031	6.40
	90	1.66	0.014	10.3
	95	1.64	0.002	32.5
PHBV/BP-L50	90	1.88	3.4	0.43
	95	1.75	2.0	0.55
	100	1.71	1.7	0.58
PHBV/BP-DL50	90	2.03	2.7	0.51
	95	1.86	3.1	0.45
	100	1.84	2.2	0.53

[a] Isothermal crystallization temperature.

Polarized microscopic analysis

The melt crystallization of neat PHBV, PHBV/BP-L50 (5 wt%), and PHBV/BP-DL50 (5 wt%) blends was further investigated using POM. A good nucleating agent decreases the activation energy required for the polymer to create a critical nucleation surface. Figure 2-5 shows the photomicrographs of the spherulite of PHBV. Polarized micrographs were taken on the 0, 2, and 60 min after quenched from melt at 180 °C. All samples showed clean and uniform melt before crystallization (0 min.). The crystallization of neat PHBV was very slow and this result accords with the isothermal crystallization behavior (Figure 2-3). The spherulite size of neat PHBV was very large, and the nuclear density was quite low. On the other hand, the addition of BP-L50 or BP-DL50 reduced the crystallization time remarkably and produced a dramatic decrease in the spherulite size and an increase in the number of spherulites relative to neat PHBV crystallized under the same conditions. During the crystallization

process, the branched poly(lactic acid) acted as a nucleating agent for PHBV, thereby increasing the nucleation density and changing the crystallization dynamics of PHBV.

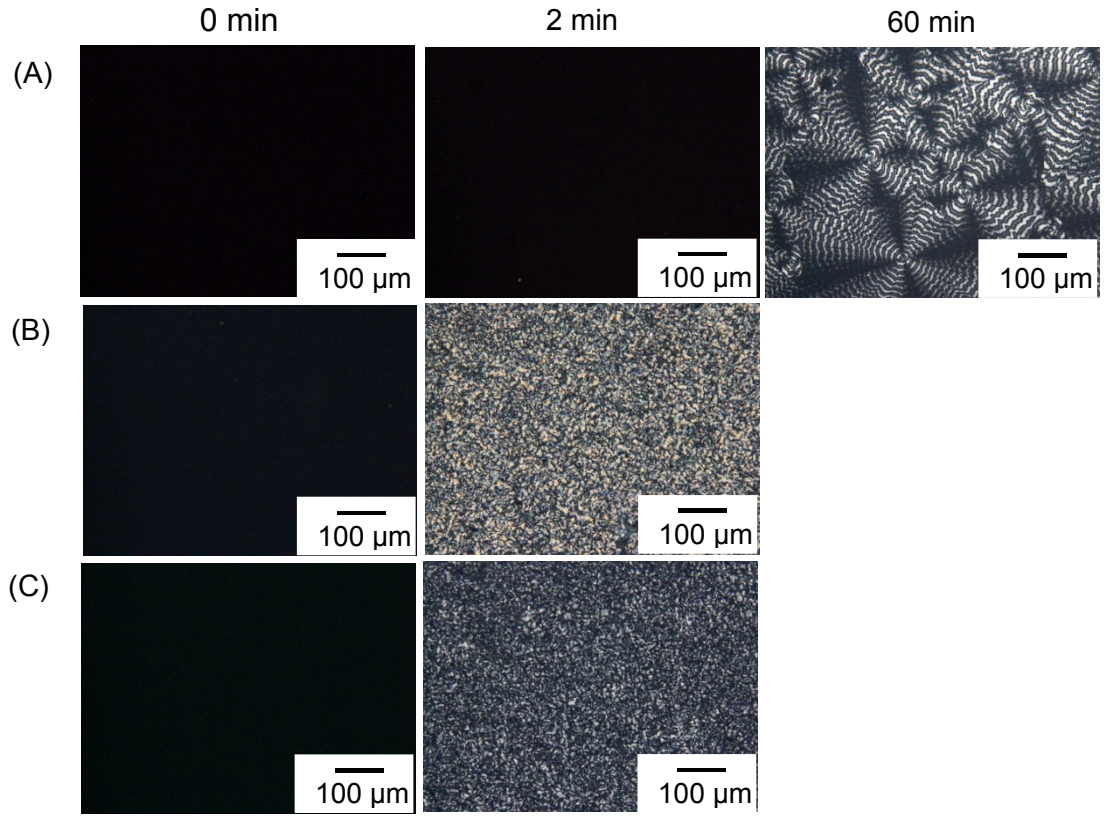

Figure 2-5 Polarized optical micrographs of (A) neat PHBV (0, 2, and 60 min), (B) PHBV/BP-L50 (5 wt%) (0 and 2 min), and (C) PHBV/BP-DL50 (5 wt%) blends (0 and 2 min).

Nucleation mechanism

In general, nucleating agents increase the crystallization rate by promoting heterogeneous nucleation. Heterogeneous nucleation utilizes foreign pre-existing surfaces to reduce the free energy of nucleation. The free energy is reduced when a nucleus contacts a pre-existing surface, leading to a smaller critical nucleus size requirement. Most nucleating agents have a melting point above 200 °C. To examine the possibility of dissolution of the branched poly(lactic acid) in the PHBV melt, microscopic observation of the PHBV/BP-L50 system was undertaken. The mixture of

PHBV/BP-L50 was heated to 180 °C on a hot stage and observed via POM. The mixture was cleanly and uniformly melted to produce a homogeneous mixture (Figure 2-5). The molecular weight and glass transition temperature of PHBV changed only marginally after heating. According to the chemical structure, a chemical reaction is not expected to occur between the branched poly(lactic acid) and PHBV, and thus the chemical nucleation can be excluded. The subsequent cooling process resulted in crystallization of PHBV (Table 2-2). These observations suggest the plausible crystallization mechanism as follows. The heterogeneous nucleation is initiated by the introduction and the phase separation of the branched poly(lactic acid). The PHBV crystal grows on the surface of the domain of the branched poly(lactic acid) in early stage. The branched poly(lactic acid), acting as a nucleating agent, decreases the surface energy barrier and increases the nucleation density for PHBV crystallization.

Conclusions

Branched poly(lactic acid)s prepared from castor oil and lactide by ring-opening polymerization were used as nucleating agents for bacterial PHBV, and the nucleating capacity of the branched poly(lactic acid)s was evaluated via differential scanning calorimetry and polarized optical microscopy. The addition of the branched poly(lactic acid) enhanced the crystallization of PHBV to allow for completion during the cooling process at 10 °C/min, whereas crystallization of the PHBV/linear poly(lactic acid) blend was not complete in same conditions. During isothermal crystallization, the crystallization rates of the PHBV/BP-L50 and PHBV/BP-DL50 blends were remarkably higher than that of neat PHBV. The branched poly(lactic acid) acted as an effective heterogeneous nucleating agent by phase separation, which promoted the crystallization remarkably and increased the crystallization rate, based on a comparison of the $t_{1/2}$ and k

values. The spherulite size of PHBV was dramatically decreased by the incorporation of the branched poly(lactic acid). These results indicate that the branched poly(lactic acid) exhibits high potential as a nucleating agent for bacterial polyesters such as PHBV.

Chapter 3

Green Composite of Poly(3-hydroxybutyrate-*co*-3-hydroxyhexanoate) Reinforced with Porous Cellulose

Introduction

Poly(3-hydroxybutyrate-*co*-3hydroxyhexanoate) (PHBH) is a copolymer consisting of randomly arranged 3-hydroxybutyrate (3-HB) and 3-hydroxyhexanoate (3-HH) units. PHBH has lower melting point and highly ductile properties than PHB. The amount of 3-HH fraction in PHBH strongly influences the properties of this polymer such as crystallinity, melting point, strength, and crystallization rate. It has been reported that the crystallinity of PHBH decreases from 60 to 18 % as 3-HH fraction increases from 0 to 25 %, making PHBH soft and flexible.[43] However, the low crystallinity results in low strength, modulus and thermal stability of PHBH and the final products are tacky due to low glass transition temperature.[44]

Composite materials are important for structural application where combination of high strength and stiffness are required.[131,132] In recent years, there is increasing interest in the development of bio-based and/or biodegradable composite materials which are sometimes called green composite.[76,133-135] One approach to make green composite is to use cellulose fibers.

Cellulose is the most abundant material in the world and about 1.5×10^{12} tons of cellulose grow every year.[136] Cellulose from wood, straw, and cotton is widely used in several industries, such as paper industry, chemical industry, textile industry, and food industry. Compared to inorganic fibers, cellulose fibers have several advantages such as renewable nature, low density, high specific strength, etc.[137,138] Cellulose fibers such as

native fibers, their fragments, and regenerated fibers were used as a reinforcement component for common polymers.[139-148] The main drawback of cellulose fibers for reinforcement applications is incompatibility with polymer matrices due to their strong hydrophilic nature. Agglomeration is a common problem when polymers are filled with cellulose fibers because of the worse adhesion between cellulose fibers and polymer matrix. Therefore, it is a major challenge how to obtain good dispersion of cellulose in polymer matrix.

Cellulose cannot be manufactured by melt processing technique and casting method in common solvent, due to the strong hydrogen bonding between intra- and inter-molecules. Therefore, many researchers have studied about solvents for cellulose. Several solvent systems such as LiCl/*N*,*N*-dimethylacetamide (DMAc), $Ca(SCN)_2$/water, LiOH/urea/water, and ionic liquids were reported and used for the modification or the preparation of cellulose gel.[149-152] This chapter deals with preparation of green composites from PHBH and porous cellulose. The porous cellulose prepared by using $Ca(SCN)_2$ aqueous solution was used as a reinforcement material, and a novel green composite from PHBH and cellulose was developed by immersion process. The resulting composites showed optically transparency with increases of mechanical properties and thermal stability.

Experimental

Materials

PHBH containing 11 mol% 3-HH (Mw= 3.2×10^5) was gift from Kaneka Co. and cellulose (Whatman CF-11) was purchased from Wako Pure Chemical Industries, Ltd. Other reagents and solvents were commercially available and were used as received.

Preparation of PHBH/cellulose composite

The following procedure was typically used in the preparation of PHBH/cellulose composites. Calcium thiocyanate ($Ca(SCN)_2$) was dissolved in deionized water to saturation (59 wt%) at room temperature. Cellulose was dispersed in this solution, and the mixture was heated at 120 ºC for 20 min to give transparent solution. The solution was cooled at room temperature to form cellulose gel. After 24 h, the gel was washed several times by ethanol, and cellulose was regenerated to porous material. For the preparation of PHBH/cellulose composite, the porous cellulose was immersed in 5 wt% of PHBH chloroform solution, followed by the drying at room temperature to remove solvent. Then, the sample was pressed at 160 °C under a pressure of 5 MPa for 5 min. This was followed by rapid quenching at 0 °C to produce PHBH/cellulose composite.

Measurements

Thermogravimetric (TG) analysis was performed using a SEIKO TG/DTA7200 (Hitachi High-Tech Science Co., Tokyo, Japan) at a heating rate of 10 °C/min under ,nitrogen. Scanning electron microscopic (SEM) analysis was carried out by a HITACHI SU-3500 instrument (Hitachi High-Technologies Co., Tokyo, Japan). The thermal properties of the samples were investigated under nitrogen atmosphere by using a SEIKO DSC6220 differential scanning calorimeter (DSC) (Hitachi High-Tech Science Co., Tokyo, Japan). The sample was melted at 180 °C for 2 min and then cooled to -50 °C at a cooling rate of 10 °C/min. The temperature was maintained for a duration of 2 min, and the sample was reached to 180 ºC at a heating rate of 10 °C/min. Polarized optical microscopic analysis was carried out using an OLYMPUS BX51 microscope (Olympus, Tokyo, Japan) equipped with an IMOTO MHS-2000 heating stage (Imoto Machinery, Kyoto, Japan). The sample was placed on a glass slide, melted at 180 °C on

a heating stage, and subsequently cooled at room temperature. Dynamic viscoelasticity analysis was carried out by using a SEIKO DMS6100 (Hitachi High-Tech Science Co., Tokyo, Japan) with frequency of 1 Hz at a heating rate of 3 °C/min. Tensile properties were measured by a Shimadzu EZ Graph (Shimadzu Co., Kyoto, Japan). A cross-head speed of 10 mm/min was used. The sample was cut into plate shape of 40 mm x 5 mm x 150 μm. Thermal expansion was measured by a SEIKO TMA/SS6100 (Hitachi High-Tech Science Co., Tokyo, Japan) in tensile mode under 10 mN tension with 10 mm span at a heating rate of 3 °C/min.

Results and discussion

Synthesis of PHBH/cellulose composite

PHBH/cellulose composite was prepared by immersion method. Porous material based on cellulose gel was used as a reinforcement filler for PHBH. Cellulose was dissolved in $Ca(SCN)_2$ aqueous solution at 120 °C, followed by cooling at room temperature to form a white cloudy gel similar to agar gel. The salt in the cellulose gel was extracted by rinsing with ethanol, and cellulose was regenerated as a white porous

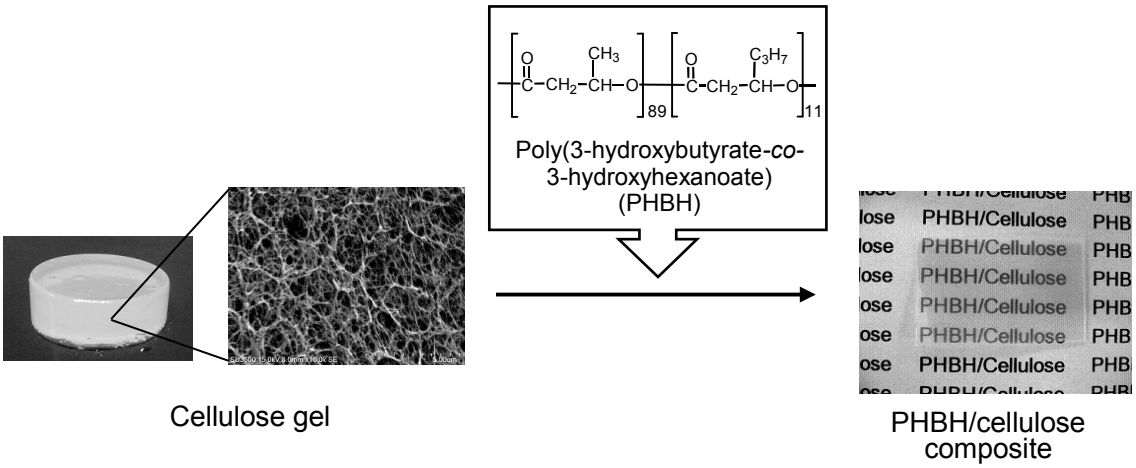

Figure 3-1. Preparation of PHBH/cellulose composite.

material retaining its shape. The formation of the porous cellulose was dependent on the cellulose concentration in $Ca(SCN)_2$ aqueous solution. The immersion method relies on penetration of dissolved PHBH into the pore of cellulose by diffusion. The regenerated cellulose with porous structure was immersed in PHBH chloroform solution, followed by the drying at room temperature to remove solvent. Figure 3-1 shows the photograph of PHBH/cellulose composite after hot pressing at 160 °C. The resulting composite was transparent and letters (PHBH/Cellulose) in the background could be seen through the sample. This result suggests structural homogeneity above visible wavelengths, resulting from the nanometric fibrous structure of cellulose. With higher cellulose content, however, some turbidity was observed, due to heterogeneous coagulation of cellulose.

TG analysis was performed to evaluate cellulose content of the composite. Figure 3-2 shows typical TG curves of neat PHBH, cellulose and PHBH/cellulose composite. The weight of neat PHBH and porous cellulose rapidly decreased at 292 and 361 ºC, respectively. The TG curves of PHBH/cellulose composites showed stepwise

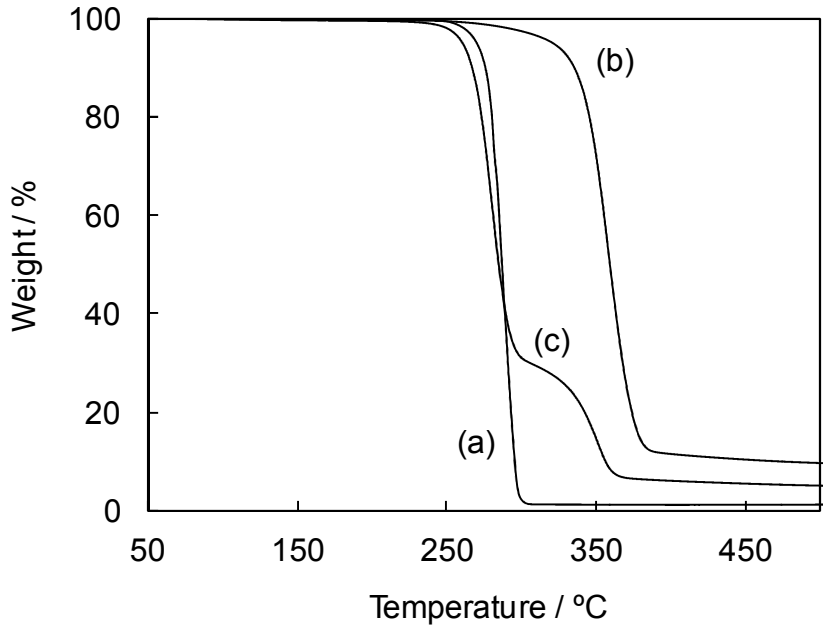

Figure 3-2. Typical TG curves of (a) neat PHBH, (b) cellulose, and (c) PHBH/cellulose-32.

degradation behaviors, and allowed assessment of cellulose content of the composite from weight decrease at ca. 360 ºC. Three composites were prepared. Sample code, cellulose concentration in $Ca(SCN)_2$ aqueous solution, cellulose content of the composites, and decomposition temperature are summarized in Table 3-1. The cellulose content depended on the cellulose concentration in $Ca(SCN)_2$ aqueous solution, indicating that the cellulose content could be controlled.

Table 3-1. Preparation of PHBH/cellulose composite

Code	Cellulose concentration[a]	Cellulose content[b]	Decomposition temperature / °C	
	/ wt%	/ wt%	T_{d1}	T_{d2}
PHBH	–[c]	0	290	–[d]
PHBH/cellulose-16	1.0	16	287	344
PHBH/cellulose-32	2.5	32	283	352
PHBH/cellulose-45	4.0	45	283	350
Cellulose	–[c]	100	–[d]	361

[a] Cellulose concentration in $Ca(SCN)_2$ aqueous solution.
[b] Cellulose content of PHBH/cellulose composite.
[c] No data.
[d] Not observed.

Figure 3-3 shows SEM images of the porous cellulose and the residue after soaking of the composite in chloroform for 24 h. The cellulose gel had highly porous structure consisting of fibrillar network, which was ascribed to the phase separation of the cellulose solution. The morphology of the residue of the composite after soaking in chloroform was similar to that of the porous cellulose, indicating that fibrillar cellulose is not aggregated during the washing by ethanol and the preparation of the composite. Furthermore, the residue weight after soaking was close to TG results.

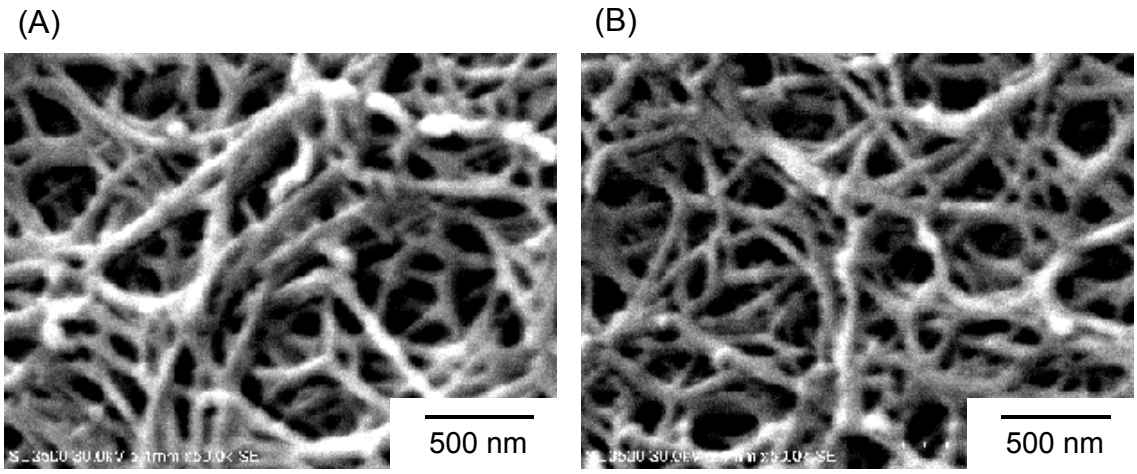

Figure 3-3 SEM images of (A) porous cellulose and (B) residue of PHBH/cellulose composite after soaking in chloroform.

Thermal properties of PHBH/cellulose composite

DSC measurement of neat PHBH and PHBH/cellulose composites was performed to evaluate the effects of the porous cellulose on thermal behaviors of PHBH (Figure 3-4). In second heating scan, glass transition, cold crystallization, and melting of PHBH were observed. The glass transition temperature (T_g) of PHBH hardly changed by the incorporation of cellulose. Similar results were reported in several studies.[153, 154] On the other hand, the cold crystallization temperature of PHBH/cellulose composites decreased and the exotherm peaks at around 40 ºC became sharper compared with that of neat PHBH. This behavior resulted because cellulose component accelerated the crystallization of PHBH. The three-dimensional network of cellulose reduced the energy barrier of nucleation to form a small critical nucleus of PHBH. Neat PHBH and PHBH/cellulose composites exhibited two melting peaks, demonstrating melting-recrystallization-melting process, the intensity of the lower melting peak of the bimodal endotherms increased by the incorporation of cellulose. This is accounted for the melting of unstable crystal and thin lamella of PHBH formed by hindrance of cellulose network. Although the crystallization of PHBH was effectively accelerated in

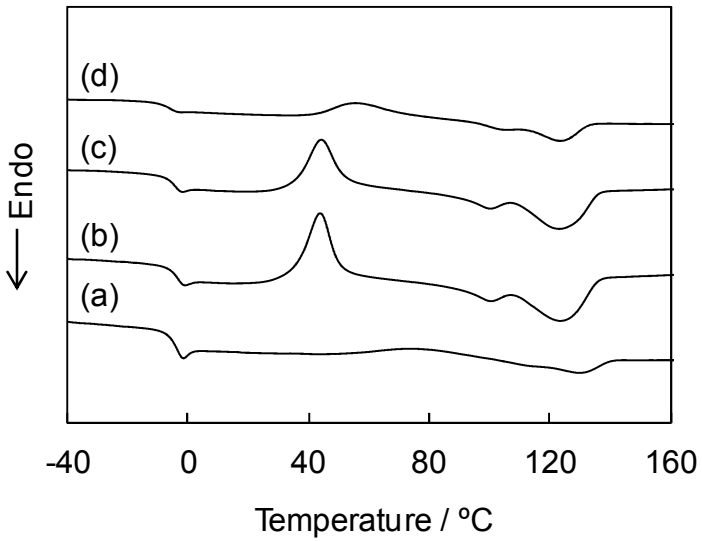

Figure 3-4. DSC curves of heating scans for (a) neat PHBH, PHBH/cellulose-16, PHBH/cellurose-32 , and (d) PHBH/cellulose-45

PHBH/cellulose-16 and PHBH/cellulose-32, the crystallization of PHBH was inhibited at higher cellulose content (PHBH/cellulose-45). This may be due to the confinement of PHBH chains caused by a large amount of cellulose.

The crystallization behaviors of PHBH were also investigated by polarized optical microscopy (Figure 3-5). Polarized optical micrographs were taken on 10 min after quenched from melt at 180 °C. In neat PHBH, the spherulite with characteristic banding and Maltese cross were observed. The spherulite size of neat PHBH was relatively large, and the nuclear density was quite low. Polarized micrograph of PHBH/cellulose composite at 180 °C showed slightly bright due to the crystallized cellulose, although fibrous structure was not observed. PHBH component crystallized during cooling process, and the porous cellulose increased the number of PHBH crystal and dramatically reduced the crystal size. These observations accord with DSC results.

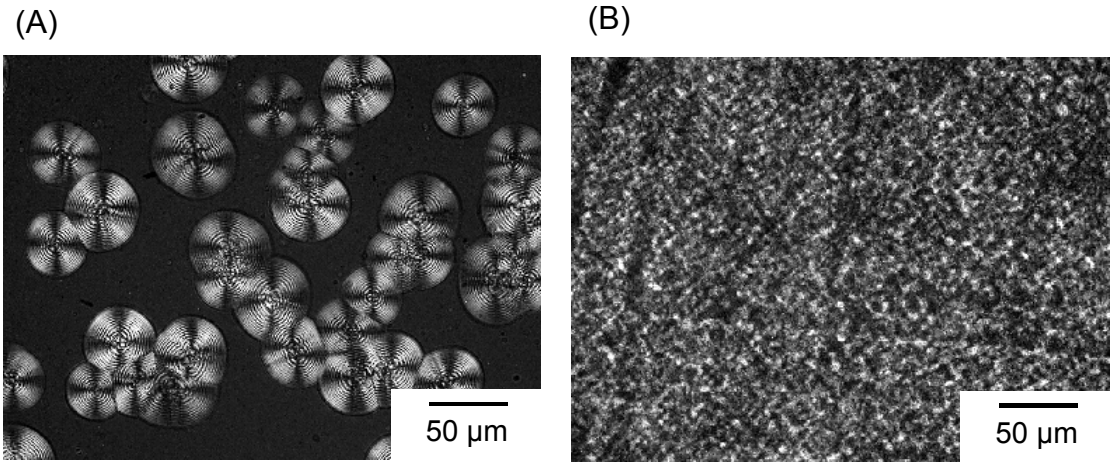

Figure 3-5. polarized optical micrographs of (A) neat PHBH and (B) PHBH/cellulose-32 composite.

Mechanical properties of PHBH/cellulose composite

To evaluate the reinforcement effect of the porous cellulose, dynamic viscoelasticity analysis was performed. Figure 3-6 shows the temperature-dependence of the storage modulus of neat PHBH and PHBH/cellulose composites. The storage modulus of neat PHBH at lower temperature (below T_g) was almost constant at around

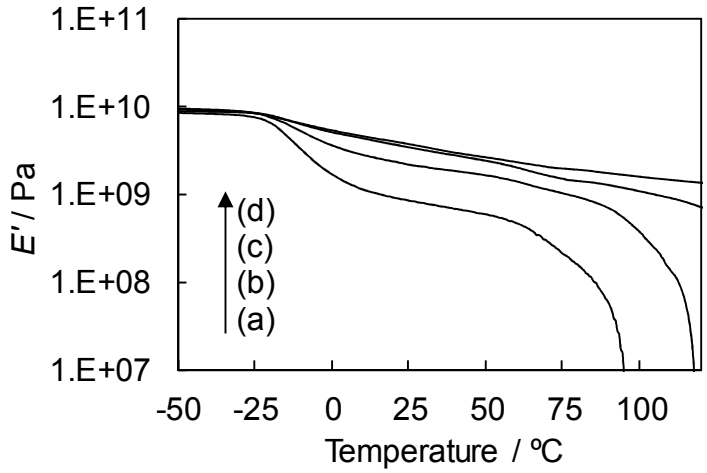

Figure 3-6. Storage modulus of (a) neat PHBH, (b) PHBH/cellulose-16, (c) PHBH/cellulose-32, and (d) PHBH/cellulose-45.

9.0 GPa and dropped at around -20 and 60 ºC, which derived from the glass transition and the melting of PHBH, respectively. The incorporation of the porous cellulose increased the storage modulus in the rubbery region and the reinforcement effect depended on the cellulose content of the composite. The storage modulus of PHBH/cellulose composites with high cellulose content was relatively higher above even the melting temperature of PHBH, suggesting the porous cellulose improved thermal stability.

The strain-stress curves of neat PHBH and PHBH/cellulose composites were shown in Figure 3-7 and the mechanical properties such as Young's modulus, maximum strength, strain at break, and toughness are summarized in Table 3-2. Mechanical properties of fiber-reinforced materials are affected on some factors such as fiber volume, aspect-ratio, fiber-matrix adhesion, and orientation. Tensile strength is dependent on the compatibility between fiber and the matrix, while modulus is influenced by fiber impregnation or aspect-ratio of fiber.[94] The Young's modulus and

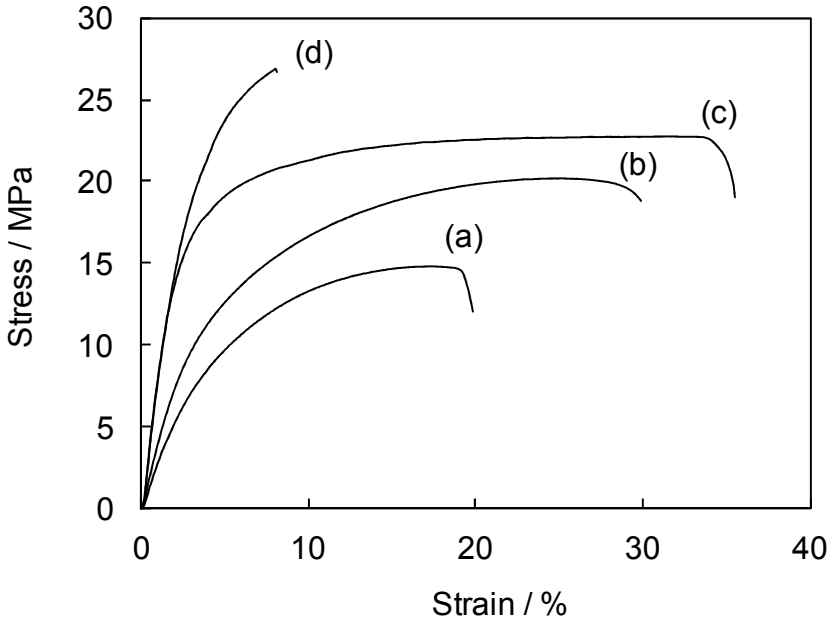

Figure 3-7. Strain-stress curves of (a) neat PHBH, (b) PHBH/cellulose-16, (c) PHBH/cellulose-32, and (d) PHBH/cellulose-45.

the tensile strength of PHBH/cellulose composites increased compared with those of neat PHBH. These behaviors are related to the three-dimensional porous structure of cellulose and the interaction between PHBH and regenerated porous cellulose owing to their relatively polar nature. These data indicate that porous cellulose acts as a reinforcement material. The strain at break of PHBH/cellulose composites was larger than that of neat PHBH. The brittleness of poly(3-hydroxyalkanoate) such as PHB and PHBH is attributed to large spherulite and secondary crystallization.[58,155)] The porous cellulose dramatically decreased the spherulite size of PHBH by the nucleating effect of cellulose. Moreover, the toughness of PHBH/cellulose-32, defined as the area of the strain-stress curve, was more than 3 times larger compared with that of neat PHBH. This data implies that the resulting composites possess a great ability to absorb energy before breaking.

Table 3-2. Mechanical properties of PHBH/cellulose composite

Code	Young's modulus / MPa	Maximum strength / MPa	Strain at break / %	Toughness / $MJ \cdot m^{-3}$
PHBH	271	15	20	2.2
PHBH/cellulose-16	378	20	29	4.9
PHBH/cellulose-32	732	22	36	7.2
PHBH/cellulose-45	746	27	8	1.5

Coefficient of thermal expansion (CTE) is reduced by the transfer of thermal stress from polymer matrix to high aspect-ratio fibrous material such as glass fiber or cellulose fiber.[156,157)] Figure3-8 shows the thermomechanical analysis results of neat PHBH and PHBH/cellulose composites. The CTEs of PHBH/cellulose composites in glassy state (below T_g) were 22-42 ppm/K, which values were smaller than that of neat PHBH. Above T_g, the CTE of neat PHBH remarkably increased. On the other hand, the incorporation of porous cellulose suppressed thermal expansion of PHBH/cellulose

composites as the cellulose content increased. These results indicate that the three-dimensional network structure of cellulose is effective in restricting thermal expansion of PHBH matrix.

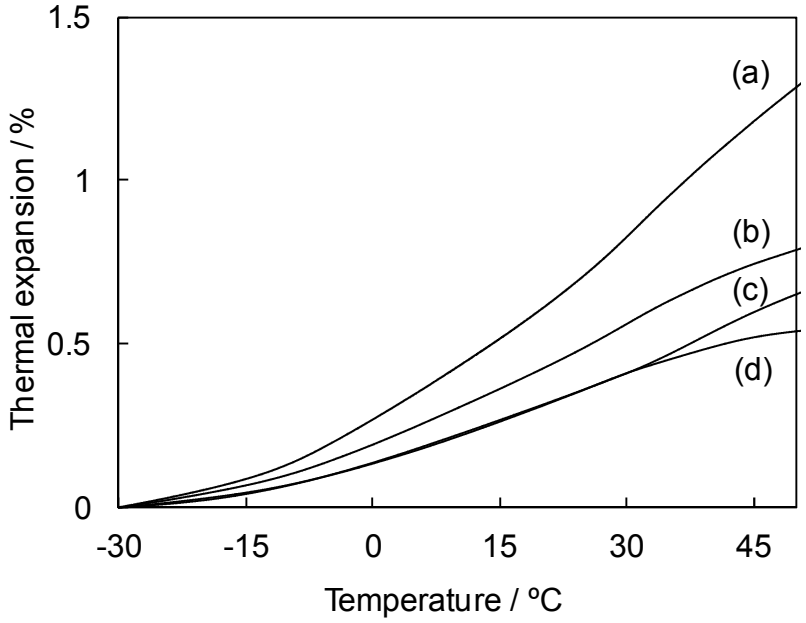

Figure 3-8. Thermal expansion of (a) neat PHBH, (b) PHBH/cellulose-16, (c) PHBH/cellulose-32, and (d) PHBH/cellulose-45.

Conclusions

A green composite from bacterial polyester and cellulose was developed, and the thermal and mechanical properties of the composite were evaluated. Regenerated porous cellulose prepared from $Ca(SCN)_2$ aqueous solution was impregnated with PHBH by immersion of the porous cellulose in polymer solution, and the subsequent drying gave a full bio-based composite. The resulting composites showed relatively good transparency due to nano-scale network structure of cellulose. The porous

cellulose accelerated the crystallization of PHBH and the spherulite size of PHBH decreased. The Young's modulus and the tensile strength of PHBH/cellulose composites were larger than those of neat PHBH. The incorporation of the porous cellulose also increased the strain at break, indicating the resulting composites are effectively reinforced without sacrificing toughness. Furthermore, the porous cellulose resulted in low thermal expansion of the composites.

Conclusion Remarks

This thesis deals with the novel bio-based materials from bacterial polyesters. The results obtained through this thesis are summarized as follows:

In Chapter 1, preparation of plant oil-based green composite using porous poly(3-hydroxybutyrate) (PHB) was mentioned. The porous PHB with topological fibrous structure was prepared by dissolution of the polymer in dimethyl sulfoxide (DMSO) by heating and the subsequent cooling, which was a simple and easy technique. The morphology and surface area of the porous PHB were dependent on the PHB concentration in DMSO. The porous PHB was impregnated with epoxidized soybean oil (ESO) by immersion, and the acid-catalyzed curing of ESO produced a full bio-based composite retaining the porous structure of PHB. The resulting composites showed relatively good transparency with reinforcement of plant oil-based network polymer. Furthermore, not only stiffness but also toughness of the composites was improved by the incorporation of the porous PHB, suggesting the good interfacial adhesion between the porous PHB and ESO polymer matrix.

In Chapter 2, the effects of branched poly(lactic acid) on crystallization of the bacterial polyester, (3-hydroxybutyrate-*co*-3-hydroxyvalerate) (PHBV) were described. The capacity of the branched poly(lactic acid) as a nucleating agent was evaluated via differential scanning calorimetry and polarized optical microscopy. Enhanced crystallization of PHBV was observed in the presence of the branched poly(lactic acid) than in linear poly(lactic acid). Crystallization of the PHBV/branched poly(lactic acid) blend from the melt was complete during the cooling process at 10 °C/min. The crystallization half time of the PHBV/branched poly(lactic acid) blend decreased significantly. By the addition of the branched poly(lactic acid), the spherulite size of

PHBV became much smaller than that of neat PHBV.

In Chapter 3, synthesis of green composite from poly(3-hydroxybutyrate-*co*-3-hydroxyhexanoate) (PHBH) and porous cellulose as a reinforcement material was described. Cellulose gel was prepared from a $Ca(SCN)_2$ aqueous solution, and the subsequent washing by ethanol gave regenerated porous cellulose without shrinkage. The PHBH/cellulose composite was fabricated by immersion of porous cellulose in a polymer solution. The cellulose content of the composites was controlled by changing the cellulose concentration of the $Ca(SCN)_2$ aqueous solution. The resulting composites showed a relatively good transparency with improvements in mechanical properties such as tensile strength, toughness, and brittleness. Furthermore, the thermal stability of the composites was improved by the incorporation of cellulose.

Given that these materials are derived from renewable resources, the biomass content of the materials from bacterial polyesters, polyhydroxyalkanoates, was 100%. Therefore, the resulting materials should contribute greatly to prevent the environmental issues such as greenhouse gas emission. This thesis provides new methodologies for the preparation of high-performance bio-based polymeric materials.

References

1) Mecking, S. *Angew. Chem. Int. Ed*. **2004**, *43*, 1078.

2) Reddy, M. M.; Vivekanandhan, S.; Misra, M.; Bhatia, S. K.; Mohanty, A. K. *Prog. Polym. Sci*. **2013**, *38*, 1653.

3) International Energy Agency: Energy Balances of OECD Countries 1999-2000, 2002.

4) Mülhaupt. R. *Macromol. Chem. Phys.* **2013**, *214*, 159.

5) General Assembly Resolution 42/187, "Report of the World Commission on Environment and Development", United Nations General Assembly 96th plenary meeting, 11th December 1987.

6) Anastas, P. T.; Warner, J. C. *Green Chemistry*, Oxford University Press, Oxford 1998.

7) Jarowenko, W.; Nostrand, S. V. *Starch-based Adhesives*, Reinhold Co., New York, 1977.

8) Imam, S. H.; Gordon, S. H.; Mao, L.; Chen, L. *Polym. Degrad. Stab*. **2001**, *73*, 529.

9) Jem, K. J.; van der Pol, J. F.; de Vos, S. *Plastics from Bacteria,* Springer-Verlag, Berlin, 2010.

10) Drumright, R. E.; Gruber, P. R.; Henton, D. E. *Adv. Mater.* **2000**, *12*, 1841.

11) Tsuji, H. *Macromol. Biosci.* **2005**, 5, 569.

12) Gupta, B.; Revagade, N.; Hilborn, *J. Prog. Polym. Sci.* **2007**, *32*, 455.

13) Lee, J.; Lee, W. *Korea-Aust. Rheol. J.* **2005**, *17*, 71.

14) Drumright, R. E.; Gruber, P. R.; Henton, D. E. *Adv. Mater.* **2000**, *12*, 1841.

15) Wang, R.; Wang, S.; Zhang, Y.; Wan, C.; Ma, P. *Polym. Eng. Sci.* **2009**, 49, 26.

16) Oksman, K. *Appl. Comp. Mater*. **2000**, *7*, 403.

17) Suprakas, S. R.; Pralay, M.; Masami, O.; Kazunobu, Y.; Kazue, U.

Macromolecules **2002**, *35*, 3104.

18) Fukuda, N.; Tsuji, H. *J. Appl. Poym. Sci.* **2005**, *96*, 196.

19) Jain, R. A. *Biomaterials* **2000**, *21*, 2475.

20) Singha, A. S. T.; Vijay, K. *Iranian- Polym. J*. **2008**, *17*, 541.

21) Holland, S. J.; Jolly, A. M.; Yasin, M.; Tighe, B. J. *Biomaterials* **1987**, *8*, 289.

22) Anderson, A. J.; Dawes, E. A. *Microbiol. Rev*. **1990**, *54*, 450.

23) Doi, Y. *Microbial Polyesters*; VCH Publishers: New York, 1990.

24) Barham, P. J.; Keller, A.; Otun, E. L.; Holmes, P. A. *J. Mater.Sci.* **1984**, *19*, 2781.

25) Lemoigne, M. *C. R. Acad. Sci.* **1923**, *176*, 1761.

26) Lemoigne, M. *C. R. Acad. Sci*. **1924**, *178*, 1093.

27) Lemoigne, M. *C. R. Acad. Sci.* **1924**, *179*, 253.

28) Lemoigne, M. *C. R. Acad. Sci.* **1925**, *180*, 1539.

29) Lemoigne, M. *Ann. Inst. Pasteur* **1925**, *39*, 144.

30) Lemoigne, M. *Bull. Soc. Chim. Biol.* **1926**, *8*, 770.

31) Lemoigne, M. *Bull. Soc. Chim. Biol.* **1927,** *9*, 446.

32) Williamson, D. H.; Wilkinson, J. F. *J. Gen. Microbiol.* **1958**, *19*, 198.

33) Doudoroff, M.; Stanier, R. Y. *Nature* **1959**, 183, 1440.

34) Wallen, L. L.; Rohwedder, W. K. *Environ. Sci. Tech.* **1974**, 8, 576.

35) Asrar, J.; Gruys, K. J. *Biodegradable Polymer (Biopol)*; Wiley-VCH, Weinheim, 2004.

36) Bohlmann, G. M. *Polyhydroxyalkanoate Production in Crops*; American Chemical Society: Washington, 2006.

37) Shimamura, K.; Kasuya, G.; Kobayashi, Y.; Shima, Y.; Doi, Y. *Macromolecules,* **1994**, *27*, 878.

38) Ballard, D. G. H.; Holmes, P. A.; Senior, P. J. *In Recent Advances in Mechanistic and Synthesis Aspects of Polymers*; *Lancaster*, Rondon, 1987.

39) Kawaguchi, Y.; Doi, Y. *Macromolecules* **1992**, *25*, 2324.

40) Chanprateep, S. J. *Biosci. Bioeng.* **2010**, *110*, 621.

41) Homes, P. A. *Phys. Technol.* **1985**, *16*, 32.

42) Doi, Y.; Tamaki, A.; Kunioka, M.; Soga, K. *Appl. Microbiol. Biotechnol.* **1988**, *28*, 330.

43) Doi, Y.; Kitamura, S.; Abe, H. *Macromolecules* **1995**, *28*, 4822.

44) Xie, Y.; Kohls, D.; Noda, I.; Schaefer, D. W.; Akpalu, Y. A. *Polymer* **2009**, *50*, 4656.

45) Sudesh, K.; Abe, H.; Doi, Y. *Prog. Polym. Sci.* **2000**, *25*, 1503.

46) Tsuge, T. J. *Biosci. Bioeng.* **2002**, *94*, 579.

47) Howells, E. R. *Chem. Ind.* **1982**, *15*, 508.

48) Inoue, Y.; Yoshie, N. *Prog. Polym. Sci.* **1992**, *17*, 571.

49) Verhoogt, H.; Ramsay, B. A.; Favis, B. D. *Polymer* **1994**, *35*, 5155.

50) He, Y.; Zhu, B.; Inoue, Y. *Prog. Polym. Sci.* **2004**, *29*, 1021.

51) Misra, S. K.; Valappil, S. P.; Roy, I.; Boccaccini, A. R. *Biomacromolecules* **2006**, *7*, 2249.

52) Chen, G. Q. *Chem. Soc. Rev*. **2009**, *38*, 2434.

53) Zhu, C.; Chiu, S.; Nakas, J.; Christopher, P.; Nomura, T. *J. Appl. Polym. Sci.* in press (DOI: 10.1002/app.39157).

54) Kai, W.; He, Y.; Asakawa, N.; Inoue, Y. *J. Appl. Polym. Sci.* **2004**, *94*, 2466.

55) Kai, W.; He, Y.; Asakawa, N.; Inoue, Y. *Polym. Int.* **2005**, *54*, 780.

56) Qian, J.; Zhu, L.; Zhang, J.; Whitehouse, R. S. *J. Polym. Sci. Part B: Polym. Phys.* **2007**, *45*, 1564.

57) Ma, P. M.; Wang, R. Y.; Wang, S. F.; Zhang, Y.; Zhang, Y. X.; Hristova, D. *J. Appl. Polm. Sci.* **2008**, *108*, 1770.

58) Pan, P.; Liang, Z.; Nakamura, N.; Miyagawa, T.; Inoue, Y. *Macromol. Biosci.* **2009**, *9*, 585.

59) Yu, F.; Pan, P.; Nakamura, N.; Inoue, Y. *Macromol. Mater. Eng.* **2011**, *296*, 103.

60) Khot, S. N.; Lascala, J. J.; Can, E.; Morye, S. S.; Williams, G. I.; Palmese, G. R.; Kusefoglu, S. H.; Wool, R. P. *J. Appl. Polym. Sci.* **2001**, *82*, 703.

61) Metzger, J. O.; Bronscheuer, U. *J. Appl. Microbiol. Biotechnol.* **2006**, *71*, 13.

62) Kumar, A.; Vemula, P. K.; Ajayan, P. M.; John, G. *Nat. Mater.* **2008**, *7*, 236.

63) Petrović, Z. S. *Polym. Rev.* **2008**, *48*, 109.

64) Swern, D.; Billen, G. N.; Findley, T. W.; Scanlan, J. T. *J. Am. Chem. Soc.* **1945**, *67*, 1786.

65) Biresaw, G.; Liu, Z. S.; Erhan, S. Z. *J. Appl. Polym. Sci.* **2008**, *108*, 1976.

66) Chakrapani, S.; Crivello, J. V. *J. Macromol. Sci. Pure Appl. Chem.* **1988**, *A35*, 1.

67) Wool, R. P. *CHEMTECH.* **1999**, *29*, 44.

68) Tran, P.; Graiver, D.; Narayan, R. *J. Appl. Polym. Sci.* **2006**, *102*, 69.

69) Tsujimoto, T.; Imai, N.; Kageyama, H.; Uyama, H.; Funaoka, M. *J. Network Polym. Jpn.* **2008**, *29*, 192.

70) Campanella, A.; La Scala, J. J.; Wool, R. P. *Polym. Eng. Sci.* **2009**, *49*, 2384.

71) Nelson, T. J.; Galhenage, T. P.; Webster, D. C. *J. Coat. Technol. Res.* **2013**, *10*, 589.

72) Tsujimoto, T.; Uyama, H.; Kobayashi, S. *Macromol. Rapid Commun.* **2003**, *24*, 711.

73) Uyama, H.; Kuwabara, M.; Tsujimoto, T.; Nakano, M.; Usuki, A.; Kobayashi, S. *Chem. Mater.* **2003**, *15*, 2492.

74) Miyagawa, H.; Misra, M.; Drazal, L. T.; Mohanty, A. K. *Polymer* **2005**, *46*, 445.

75) Lligadas, G.; Randa, J. C.; Galia, M.; Cádiz, V. *Biomacromolecules* **2006**, *7*, 3521.

76) Tsujimoto, T.; Uyama, H.; Kobayashi, S. *Polym. Degrad. Stab.* **2010**, *95*, 1399.

77) Williams, G. I.; Wool, R. P. *Appl. Composite Mater.* **2000**, *7*, 421.

78) Rakotonirainy, A. M.; Padua, G. W. *J. Agric. Food Chem.* **2001**, *49*, 2860.

79) Shibata, M.; Teramoto, N.; Someya, Y.; Suzuki, S. *J. Polym. Sci. Part B: Polym. Phys.* **2009**, *47*, 669.

80) Tsujimoto, T.; Ohta, E.; Uyama, H. *J. Network Polym. Jpn.* **2013**, *34*, 85.

81) Imai, N.; Kageyama, H.; Uyama, H. *Chem. Lett.* **2007**, *36*, 698.

82) Xin, Y.; Uyama, H. *Chem. Lett*. **2012**, *41*, 1509.

83) Kistler, S. S. *Nature* **1931**, *127*, 741.

84) Hüsing, N.; Schubert, U. *Angew. Chem. Int. Ed.* **1998**, *37*, 22.

85) Mayr, M.; Mayr, B.; Buchmeiser, M. R. *Angew. Chem. Int. Ed.* **2001**, *40*, 3839.

86) Shih, Y. H.; Singco, B.; Liu, W. L.; Hsu, C. H.; Huang, H. Y. *Green Chem.* **2011**, *13*, 296.

87) Isobe, N.; Sekine, M.; Kimura, S.; Wada, M.; Kuga, S. *Cellulose* **2011**, *18*, 327.

88) Kadokawa, J.; Takegawa, A.; Mine, S.; Prasad, K. *Carbohydr. Polym.* **2011**, *84*, 1408.

89) Okada, K.; Nandi, M.; Maruyama, J.; Oka, T.; Tsujimoto, T.; Kondoh, K.; Uyama, H. *Chem. Commun.* **2011**, *47*, 7422.

90) Liu, S.; Yan, Q.; Tao, D.; Yu, T.; Liu, X. *Carbohydr. Polym.* **2012**, *89*, 551.

91) Hayase, G.; Kanamori, K.; Hasegawa, G.; Maeno, A.; Kaji, H.; Nakanishi, K. *Angew. Chem. Int. Ed.* **2013**, *52*, 10788.

92) Agrawal, M.; Gupta, S.; Zafeiropoulos, N. E.; Oertel, U.; Häßler, R.; Stamm, M. *Macromol. Chem. Phys.* **2010**, *211*, 1925.

93) Fahma, F.; Hori, N.; Iwata, T.; Takemura, A. *J. Appl. Polym. Sci.* **2013**, *130*, 1563.

94) Eichhorn, S. J.; Baillie, C. A.; Zafeiropoulos, N.; Mwaikambo, L. Y.; Ansell, M. P.; Dufrense, A.; Entwistle, K. M.; Herrera-Franco, P. J.; Escamilla, G. C.;

Groom, L.; Hughes, M.; Hill, S. C.; Rials, T. G.; Wild, P. M. *J. Mater. Sci.* **2001**, 31, 2107.

95) Cecorulli, G.; Pizzoli, M.; Scandola, M. *Macromolecules* **1992**, *25*, 3304.

96) Ishiaku, U. S.; Shaharum, A.; Ismail, H.; Mohd Ishak, Z. A. *Polym. Int.* **1997**, *45*, 83.

97) Choi, J. S.; Park, W. O. *Polym. Test.* **2004**, *23*, 455.

98) Robertson, M. L.; Chang, K.; Gramlich, W. M.; Hillmyer, M. A. *Macromolecules*, **2010**, *43*, 1807.

99) Grassie, N.; Murray, E. J.; Holmes, P. A. *Polym. Degrad. Stab.* **1984**, *6*, 95.

100) Barham, P. J.; Keller, A. J. *Polym. Sci. Part B: Polym. Phys.* **1986**, *24*, 69.

101) de Koning, G. J. M.; Lemstra P. J. *Polym*er **1993**, *34*, 4089.

102) Hobbs, J. K.; McMaster, T. J.; Miles, M. J.; Barham, P. J. *Polym*er **1996**, *37*, 3241.

103) Steinbüchel, A.; Füchtenbusch, B. *Trends in Biotechnol*. **1998**, *16*, 419.

104) El-Hadi, A.; Schnabel, R.; Straube, E.; Müller, G.; Henning, S. *Polym. Test.* **2002**, *21*, 665.

105) Avella, M.; Martuscelli, E. *Polymer* **1988**, *29*, 1731.

106) Cavallaro, P.; Immirzi, B.; Malinconico, M.; Martuscelli, E.; Volpe, M. I. *Macromol. Rapid Commun.* **1994**, *15*, 103.

107) Zhang, L.; Xiong, C.; Deng, X. *Polymer* **1996**, *37*, 235.

108) Saito, M.; Inoue, Y.; Yoshie, N. *Polymer* **2001**, *42*, 5573.

109) Zhang, J.; McCarthy, S.; Whitehouse, R. *J. Appl. Polym. Sci*. **2004**, *94*, 483.

110) Liu, W. J.; Yang, L. H.; Wang, Z.; Dong, L. S.; Liu, J. J. *J. Appl. Polym. Sci.* **2002**, *86*, 2145.

111) Barham, P. J. *J. Mater. Sci*. **1983**, *19*, 3826.

112) Organ, S. J.; Barham, P. J. *J. Mater. Sci.* **1984**, *26*, 1368.

113) Black, S. N.; Dobbs, B.; Dempsey, P. S.; Davey, R. J. *J. Mater. Sci. Lett.* **1990**,

9, 51.

114) Organ, S. J.; Barham, P. J. *J. Mater. Sci.* **1992**, *27*, 3239.

115) Avella, M.; Martuacelli, E.; Raimo, M. *Polymer* **1993**, *34*, 3234.

116) Csomorová, K.; Rychlý, J.; Bakoš, D.; Janigová, I. *Polym. Degrad. Stab.* **1994**, *43*, 441.

117) Withey, R. E.; Hay, J. N.; Hammond, T. *Polymer* **1999**, *40*, 5147.

118) Choi, W. M.; Kim, T. W.; Park, O. O.; Chang, Y. K.; Lee, J. W. *J. Appl. Polym. Sci*. **2003**, *90*, 525.

119) He, Y.; Inoue, Y. *Biomacromolecules* **2003**, *4*, 1865.

120) Lai, M.; Li, J.; Yang, J.; Liu, J.; Tong, X.; Cheng, H. *Polym. Int.* **2004**, *53*, 1479.

121) He, Y.; Inoue, Y. *J. Polym. Sci.: Part B: Polym. Phys.* **2004**, *42*, 3461.

122) Tsujimoto, T.; Haza, Y.; Yin, Y.; Uyama, H. *Polym. J.* **2011**, *43*, 425.

123) Kawaguchi, Y.; Doi, Y. *FEMS Microbiol. Lett.* **1990**, *70*, 151.

124) Mishra, S. P.; Deopura, B. L. *Makromol. Chem.* **1985**, *186*, 641.

125) Hsu, W. P. *J. Appl. Polym. Sci.* **2002**, *83*, 1425.

126) Avrami, M. *J. Chemical Phys.* **1939**, *7*, 1103.

127) Avrami, M. *J. Chem. Phys.* **1940**, *8*, 212.

128) Avrami, M. *J. Chem. Phys.* **1941**, *9*, 177.

129) Wunderlich, B. *Macromolecular Physics. Vol. 2*; Academic Press: New York, 1976.

130) Hiemenz, P. *Polymer Chemistry*; Marcel Deckker: New York, 1984.

131) Hussain, F.; Hojjati, M.; Okamoto, M.; Gorga, R. E. *J. Compos. Mater.* **2006**, *40*, 1511.

132) Sun, X.; Sun, Y.; Li, H.; Peng, H. *Adv. Mater.* **2013**, *25*, 1.

133) Lezak, E.; Kulinski, Z.; Masirek, R.; Piorkowska, E.; Pracella, M.; Gadzinowska, K. *Macromol. Biosci*. **2008**, *8*, 1190.

134) Nyambo, C.; Mohanty, A. K.; Misra, M. *Biomacromlecules* **2010**, *11*, 1654.

135) Koronis, G.; Silva, A.; Fontul, M. *Compos. Part B.* **2013**, *44*, 120.

136) Abdul Khalil, H. P. S.; Bhat, A. H.; Irena Yusra, A. F. *Carbohydr. Polym.* **2012**, *87*, 963.

137) Saheb, D. N.; Jog, J. P. *Adv. Polym. Technol.* **1999**, *18*, 351.

138) Bledzki, A. K.; Gassan, J. *Prog. Polym. Sci.* **1999**, *24*, 221.

139) Espert, A.; Camacho, W.; Karlson, S. *J. Appl. Polym. Sci.* **2003**, *89*, 2353.

140) Shanks, R. A.; Hodzic, A.; Wong, S. *J. Appl. Polym*. *Sci*. **2004**, *91*, 2114.

141) Iwamoto, S.; Nakagaito, N. A.; Yano, H.; Nogi, M. *Appl. Phys. Part A.* **2005**, *81*, 1109.

142) Bhardwaj, R.; Mohanty, A. K.; Drzal, L. T.; Pourboghrat, F.; Misra M. *Biomacromolecules* **2006**, *7*, 2044.

143) Bondeson, D.; Oksman, K. *Compos. Part A.* **2007**, *38*, 2486.

144) Zini, E.; Focarete, M. L.; Noda, I.; *Compos. Sci. Technol.* **2007**, *67*, 2085.

145) Cao, X.; Dong, H.; Li, C. M. *Biomacromolecules* **2007**, *8*, 899.

146) Suryanegara, L.; Nakagaito, A. N.; Yano, H. *Compos. Sci. Technol*. **2009**, *69*, 1187.

147) Endo, R.; Saito, T.; Isogai, A. *Polymer* **2013**, *54*, 935.

148) Mullera, D.; Rambo, C. R.; Porto, L. M.; Schreinerd, W. H.; Barra, G. M. O. *Carbohydr. Polym.* **2013**, *94*, 655.

149) Kuga, S. *J. Colloid Interface Sci.* **1980**, *77*, 413.

150) McCormick, C. L.; Callais, P. A.; Hutchinson, B. H. Jr. *Macromolecules* **1985**, *18,* 2394.

151) Swatloski, R. P.; Spear, S. K.; Holbrey, J. D.; Rogers, R. D. *J. Am. Chem. Soc*. **2002**, *124*, 4974.

152) Cai, J.; Zhang, L. *Macromol. Biosci.* **2005**, *5*, 539.

153) Hajji, P.; Cavaille, J. Y.; Favier, V.; Gauthier, C.; Vigier, G. *Polym. Compos*.

1996, *17*, 612.

154) Ten, E.; Turtle, J.; Bahr, D.; Jiang, L.; Wolcott, M. *Polymer* **2010**, *51*, 2652.

155) Puente, J. A. S.; Esposito, A.; Chivrac, F.; Dargent, E. *Macromol. Symp*. **2013**, *328*, 8.

156) Segal, L. *Polym. Eng. Sci.* **1979**, *19*, 365.

157) Shimazaki, Y.; Miyazaki, Y.; Takezawa, Y.; Nogi, M.; Abe, K.; Ifuku, S.; Yano, H. *Biomacromolecules* **2007**, 8, 2976.

List of Publications

1. Phase Separation-induced Crystallization of Poly(3-hydroxybutyrate-*co*-hydroxyvalerate) by Branched Poly(lactic acid)
   Nao Hosoda, Eun-Hye Lee, Takashi Tsujimoto, Hiroshi Uyama
   Industrial & Engineering Chemistry Research, **2013**, *52*, 1548-1553.

2. Green Composite of Poly(3-hydroxybutyrate-*co*-3-hydroxyhexanoate) Reinforced with Porous Cellulose
   Nao Hosoda, Takashi Tsujimoto, Hiroshi Uyama
   ACS Sustainable Chemistry & Engineering, **2014**, *2*, 248-253.

3. Plant Oil-based Green Composite Using Porous Poly(3-hydroxybutyrate)
   Nao Hosoda, Takashi Tsujimoto, Hiroshi Uyama
   Polymer Journal, in press (DOI:10.1038/pj.2014.1).

Acknowledgements

The present research was carried out from 2011 to 2014 at Department of Applied Chemistry, Graduate School of Osaka University.

First of all, I would like to thank my supervisor, Professor Dr. Hiroshi Uyama for his invaluable guidance, discussion and kind heart supports throughout this research.

I would like to express thanks to Professor Dr. Susumu Kuwabata and Professor Dr. Takahiro Kozawa for their valuable comments and suggestions.

I deeply thank Assistant Professor Dr. Takashi Tsujimoto. His critical and appropriate advices always led me to much success in my research. With him, I enjoyed my research and tried to develop new ideas.

I would like to express my gratitude to Assistant Professor Dr. Urara Hasegawa and Dr. André J. van der Vlies for their valuable comments.

I would like to thank Professor Dr. Jun-ichi Azuma and Associate Professor Dr. Junji Sakamoto for their valuable discussion.

I deeply thank Dr. Yasushi Takeuchi for his important advices, discussion and hearty encouragement.

Furthermore, I would like to thank Dr. Eun-Hye Lee, Ms. Sung-Bin Park, Ms. Xiaoxia Sun, Ms. Yoshimi Haza, Ms. Emi Ohta, Mr. Shumpei Nishio, Mr. Hiroki Tsushima, Ms. Hyun-Hee Shim, Mr. Ken-ichi Toshimitsu, Mr. Kazuki Chujo, Mr. Takuya Yamauchi, Mr. Yusuke Yukino, and all the other members of Uyama Laboratory for their kind help. I could have very nice and precious three years with them.

Finally, I am particularly grateful to my mother, Mrs. Taeko Hosoda, and to my brother, Mr. Jun Hosoda, for their understanding and constant supports. Without their encouragement, I could never have achieved this research.

January, 2014

Nao Hosoda